
WESTERN SYDNEY
UNIVERSITY
NSW
GOVERNMENT
MACQUARIE
University
SYDNEY·AUSTRALIA
SCHOOL
MICROCLIMATES
SEPTEMBER 2020

AUTHORS

Sebastian Pfautsch, Susanna Rouillard, Agnieszka Wujeska-Klause, Art Bae, Lyn Vu
Urban Studies
School of Social Sciences

Kathryn Holmes
School of Education

Western Sydney University, Parramatta, NSW 2150, Australia

Michelle Leishman, Leigh Staas, Anthony Manea, Samiya Tabassum, Alessandro Ossola
Department of Biological Sciences & Smart Green Cities

Macquarie University, NSW 2109, Australia

This research project has been funded by the Department of Planning, Industry and Environment, Government of New South Wales, Western Sydney University and Macquarie University.

With respect for Aboriginal cultural protocol and out of recognition that its campuses occupy their traditional lands, the Darug, Tharawal (also historically referred to as Dharawal), Gandangara and Wiradjuri peoples are acknowledged and thanked for their support of its work in their lands (Greater Western Sydney and beyond).

The authors acknowledge the support of the project by the New South Wales Department of Education and generous in-kind support by Orora Group Australia.

Suggested citation:
Pfautsch S., Rouillard S., Wujeska-Klause A., Bae A., Vu L., Manea A., Tabassum S., Staas, L., Ossola A., Holmes, K. and Leishman M. (2020) School Microclimates. Western Sydney University, 56 p.

DOI: https://doi.org/10.26183/np86-t866

www.westernsydney.edu.au

September, 2020.

Cover and other images from istock.com and unsplash.com

SYNOPSIS

Outdoor school environments need to be safe, stimulate physical and cognitive development of children and encourage learning. These key requirements are jeopardised by increasing summer heat. Summer heat limits outdoor activities and has adverse effects on physical wellbeing of school children and teachers. Children are particularly vulnerable to heat as they regulate their core temperature through convection, which becomes less effective when it is hot. It is thus increasingly important to protect children from summer heat, which is predicted to become more frequent and intense as a result of global warming.

One important requirement of preventing a decline in educational outcomes and rising risk of physical harm during periods of intense summer heat is a sound understanding of school microclimates and options to cool these environments down. To date, evidence-based design and building guidelines to effectively mitigate heat and create cool outdoor environments in schools of NSW and across Australia are missing.

The present work is part of the Cool Schools initiative led by Western Sydney University in conjunction with the NSW Government. It provides guidance on how to reduce the impacts of heat on school outdoor environments. The present report is intended as guideline for those that plan, design, maintain and manage schools. The goal of the initiative is to inform how resilience of schools against summer heat can be improved, thereby increasing child safety and extending the time for outdoor learning and play in summer. Understanding how common building and surface materials can intensify heat and quantifying the cooling effect of shade are the first steps towards achieving this goal.

For this purpose, microclimates around a school in Western Sydney, NSW, Australia, were studied during summer 2019-20 (17 December 2019 to 26 January 2020), the hottest summer on record since 1910. The project took place during the summer holidays for two reasons: (1) preventing damage or loss of scientific equipment and (2) to record data during hot conditions that become increasingly common during summer when schools are open. Air and 'feels like' temperatures were recorded around buildings, the school yard, gardens, tree groves, open spaces and a playground. Surface temperatures of sunlit and shaded asphalt, concrete, bare soil, artificial grass and green turf were measured. The area of shade provided by trees was quantified, and their water use was determined.

When unshaded, the surface temperature of bare soil rose above 70°C. Unshaded asphalt, the dominant surface material of the central school yard, reached similar temperatures and 'feels like' temperatures reached 55°C above this surface. Artificial grass displayed the highest mean surface temperatures during days with normal, hot and extreme air temperatures. Shading these surfaces markedly reduced their surface temperature by up to 20°C, which in turn lowered 'feels like' temperatures by 10°C and thus improved human thermal comfort.

More than 100,000 data points from 20 locations around the school were used to generate novel microclimate maps that visualise variation of summer air temperature across outdoor environments of the entire school. Additional maps focussed on the time intervals of morning recess and lunch time when children would gather and play in these environments. The maps allowed to identify cool and hot zones. Using maps like these can assist school managers and teachers to develop heat-smart play strategies. Moreover, once hot zones have been identified, actions can be initiated to mitigate heat.

The lowest air and surface temperatures were consistently recorded under tree canopies. This highlights the importance of canopy cover to cooling down school microclimates. Generating these cooling benefits depends on tree species, canopy size and availability of soil moisture. Daily water use of a banksia (*Banksia integrifolia*) was 9 litres. Low water use indicates low evaporative cooling benefits. The tree also had a small and open canopy (<20 m^2), providing little shade to reduce surface temperatures. A large Queensland brush box tree (*Lophostemon confertus*) consumed 156 litres per day and provided 170 m^2 of shade, which resulted in valuable cooling benefits

Understanding species-specific differences related to canopy size and water use allows selection of tree species that generate maximal thermal benefits in schools. Based on 7 key criteria related to cooling and safety, Jacaranda (*Jacaranda mimosifolia*) and Weeping Lilly Pilly (*Syzygium floribundum*) were the most appropriate tall trees, whereas Weeping Bottlebrush (*Callistemon viminalis*) and Queensland Brush Box (*Lophostemon confertus*) were ideal shorter tree species.

This report provides more than 20 practical recommendations on how to reduce the impacts of outdoor heat. Although these recommendations were devised based on work around a public school in Western Sydney, their universal character allows applying them to any school and other build environment. Avoiding the use of artificial grass in unshaded spaces, shading black asphalt, allowing natural air flows and using shade materials with highly reflective upper surfaces should be fundamental principles in design and building guidelines for heat-smart schools.

Increasing summer heat represents a hazard for children. Creating cool outdoor spaces in schools where children can learn and play safely during summer must become standard. This report will assist in working towards this target.

CONTENTS

COOL SCHOOLS CRIB SHEET

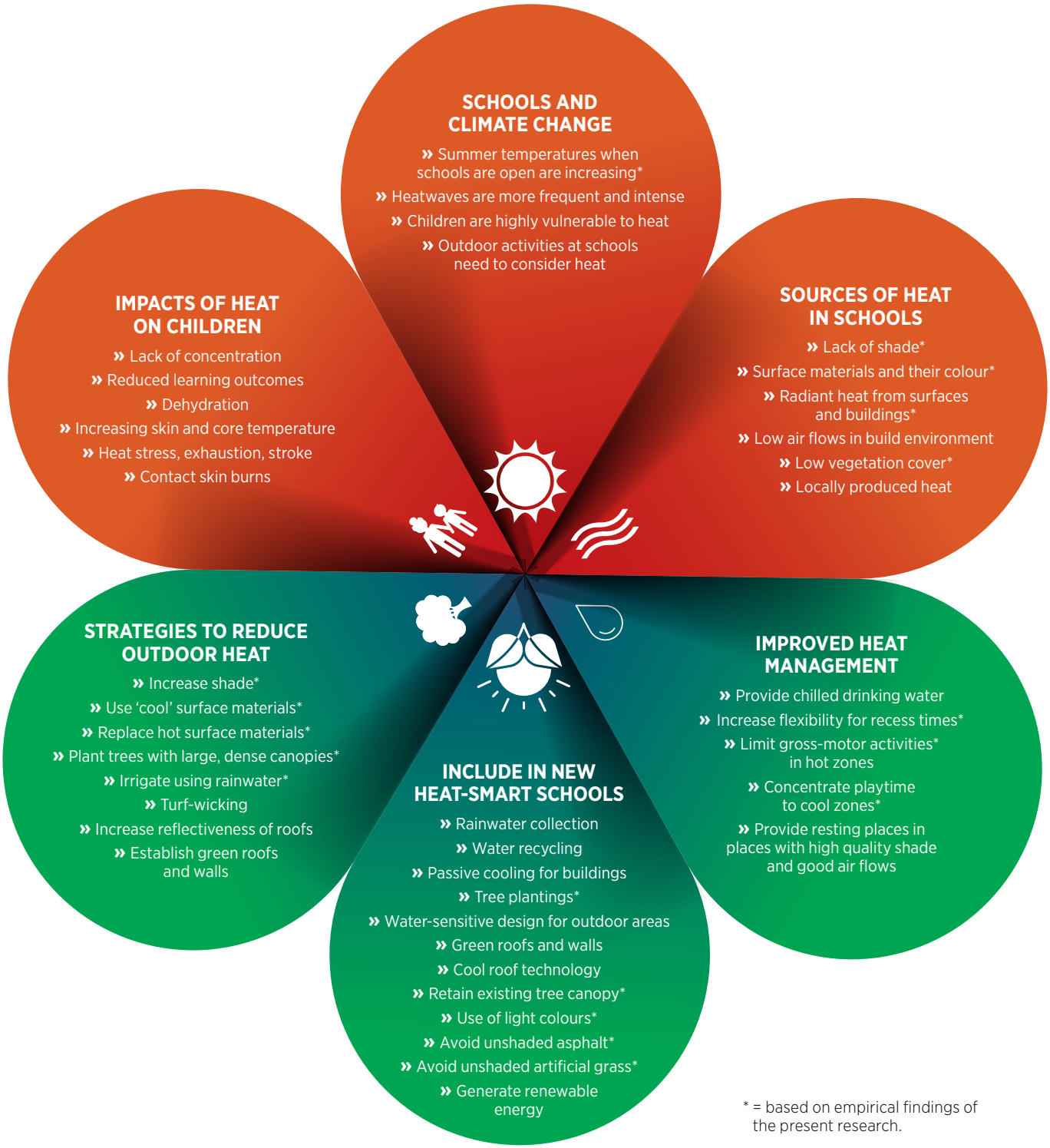

* = based on empirical findings of the present research.

1. BACKGROUND

1.1 HEAT AND LEARNING

The negative effect of heat on learning outcomes applies globally (Fig. 1). There are indirect and direct drivers for this relationship. Indirect factors include insufficient nutrition, poor health or the inability to pay school fees, which is generally greater in warmer countries (see Goodman et al. 2018 and references therein). The direct and negative effect of heat on learning outcomes has been established in both controlled experiments (Seppänen et al., 2006) and field studies (Cedeño Laurent et al., 2017).

Ambient air temperatures around 22.5°C represent optimal learning conditions in classrooms of Australia (de Dear et al., 2015). Warmer (and also cooler) temperatures have been found to impact decision making and cause substantial discomfort, affecting short-term cognition and work performance (Seppänen et al., 2006; Wargocki et al., 2010). These effects can impact both students and teachers. A comprehensive, long-term study on the impacts of temperature on learning in schools found that with every degree Celsius increase in annual mean classroom temperature above optimal learning temperatures, schoolyear learning outcomes decrease by 2% (Goodman et al., 2018).

Air temperature in classrooms can be regulated and air conditioning systems will help to lower classroom temperatures during summer. However, many classrooms and entire schools in NSW and across Australia do not have access to air conditioning and rely on ceiling fans and natural ventilation. The effectiveness of fans and natural ventilation declines once ambient air temperatures increase. Hence, learning conditions of pupils during summer are currently not equal throughout Australia.

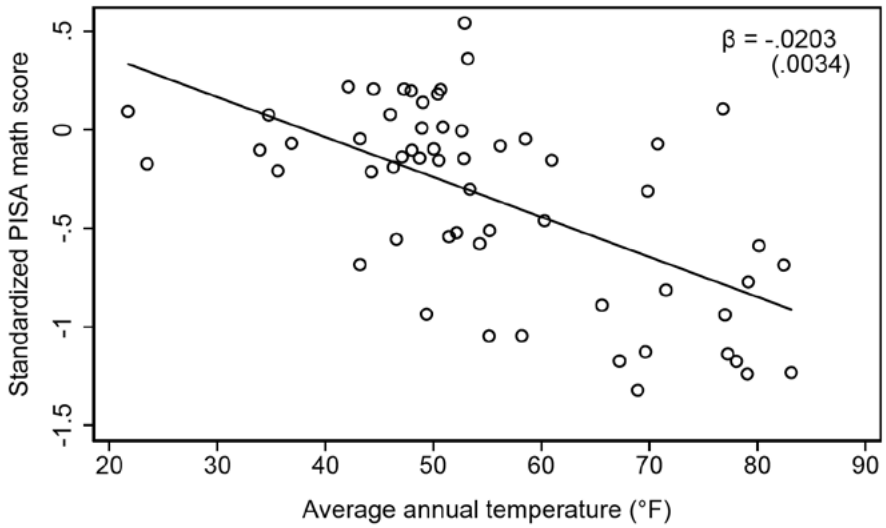

FIGURE 1: Standardised Program for International Student Assessment (PISA) math scores of 2012 from 60 countries around the world. Mean annual temperature for each country was calculated for the years 1980 to 2011. The solid line shows the linear fit of the bivariate regression between temperature and PISA scores. The slope coefficient of the regression is also shown. Figure from Goodman et al. (2018).

International studies demonstrate the consequences of this situation. In the United States, schools that did not have air-conditioning saw reading scores improve markedly after air conditioning upgrades (Neilson and Zimmerman, 2014). Improvements of between 5 and 10% in reading and math scores were documented for school children that moved from a school without adequate cooling to a new-build school where adequate cooling was provided (Lafortune and Schonholzer, 2018).

As response to the lack of comprehensive studies of the impacts of heat on learning outcomes in Australia, Western Sydney University commenced its *Cool Schools* initiative in 2018. The first output of the *Cool Schools* initiative was a comprehensive report (Madden et al., 2018) that reviewed current policies and practices around heat and learning, provided an overview on legislation, building codes, standards, sustainability education and innovative trends in building and landscape design (Fig. 2).

FIGURE 2: The *Cool Schools* report was published by Madden and colleagues in 2018. The document is publicly available at: https://doi.org/10.26183/5b91d72db0cb7.

In the same year that the *Cool Schools* Report was published, an article by Baker and Gladstone (2018) in the Sydney Morning Herald reported that, based on data from the NSW Department of Education, around 10,000 classrooms in NSW had no air conditioning. In recognition of increasing heat in summer and resulting impacts on students that learn in classrooms without air-conditioning, the NSW Government initiated the 'Cooler Classrooms Program'. The program is a $500 million initiative to provide air conditioning to classrooms and libraries. In the first round of assessments in 2018, 900 schools were approved to receive air conditioning.

The objective of the Cooler Classrooms Program is to improve learning outcomes and thermal comfort of students by improving indoor ventilation and air quality (NSW Department of Education, 2018). Schools with a mean maximum January temperature at or above 30°C are eligible to have air conditioning systems installed. Delivering this vital program to provide equal learning opportunities across the state of NSW is difficult for a number of reasons (e.g., supply capacity of local electricity grids, building heritage aspects and structural support). By the end of 2018, upgrades at around 30 schools were finalised and work was underway at many more.

1.2 HEAT AND HEALTH

While heat influences learning and educational outcomes, it also represents a serious health risk. Historically, extreme heat in Australia has claimed more lives than all other natural disasters combined (Coates et al., 2014). During times of high or extreme heat, the risk of dehydration and associated impairment of cognitive functioning, heat stress, heat exhaustion and heat stroke rises exponentially (Atha, 2013; Vanos, 2014).

Physical activities during high ambient temperatures accelerate fluid imbalance and raise skin and core temperatures (hyperthermia), thereby exerting additional strain on the cardiovascular system (Morrison and Sims, 2014).

Educational institutions such as schools are particularly vulnerable to heat as their young occupants are yet to learn how to self-assess signs of increasing heat stress and their options to improve thermal comfort through behavioural adjustment (Teli et al., 2017). The core temperature of children seems to depend largely on ambient temperature and less on solar radiation (Hanatani et al., 2011). This effect is a consequence of the larger surface area-to-mass ratio in children compared to adults. Generally, children achieve heat loss through radiation and convection (dry heat loss) in contrast to evaporative cooling (sweating) that adults are capable of. Dry heat loss is less effective in high temperature environments, and nearly ceases when experiencing humid heat. This highlights the sensitivity of children to their physical environment (Teli et al., 2012).

Not to be underestimated is the potential burn hazard from hot surface materials. The ISO 13732 (2010) *Burn Thresholds of Skin* defines surface temperatures and contact times for materials that are commonly found in outdoor school environments. For example, contact time of more than 5 seconds with concrete or asphalt that is 60°C is regarded hazardous. The contact time is reduced to 3 seconds when touching coated metal with a surface temperature of 65°C. Contact thermal conductance of materials dictate the intensity and duration of heat transfer from the material into skin, which explains why it is safe to touch uncoated wood with a surface temperature of 93°C for about 5 seconds. Contact times are likely to be less for children with thinner epidermis of palms and soles when compared to adults (Oliveria et al., 2006).

1.3 **OUTDOOR HEAT**

Every school is more than its classrooms. While the majority of learning takes place inside the classroom, important activities, including sport and play take place outside the classroom. In addition, the value of regular outdoor learning activities in schools is increasingly recognised (Harris, 2017). Moreover, wellbeing of school children is influenced by outdoor activities during recess times where active play promotes general physical and mental health and stimulates the development of cognitive, social and emotional abilities (Brockman et al., 2011). Morning recess and lunch break can comprise up to 20% of the time spent at school every day and nearly one quarter of the total daily physical activity of children takes place during these two intervals (Ridgers et al., 2013).

As the daily time that children spend doing physical activity is generally decreasing (Ridgers et al., 2013), outdoor activities during morning recess and lunch break become even more important to harness the multitude of benefits from active play (Brockman et al., 2011). Yet, most school outdoor environments are not designed with the specific aim to protect and improve thermal comfort and heat safety of children. In addition, increasing frequency and intensity of extreme summer heat as a result of climate change (Varduolakis et al. 2014) creates hazardous conditions that threaten the wellbeing of children and teachers even in well-designed outdoor spaces. In response to these conditions, time for outdoor activities is reduced, which leads to a further decrease in physical activity and a promotion of more sedentary learning and play activities.

The Climate Statement of the Bureau of Meteorology for 2019 documents a grim reality when it comes to heat (www.bom.gov.au/climate/current/annual/aus/#tabs=Temperature):

- Nine of the ten hottest years recorded in Australia have occurred after 2005
- 2019 was the hottest ever recorded in Australia, with 1.52°C above long-term (1961-1990) mean air temperatures
- In NSW, 11 of the hottest years have occurred after 2005
- 2019 was the hottest year in NSW where temperatures were nearly 2°C above the long-term mean
- Maximum temperatures in NSW were 2.44°C above the long-term mean

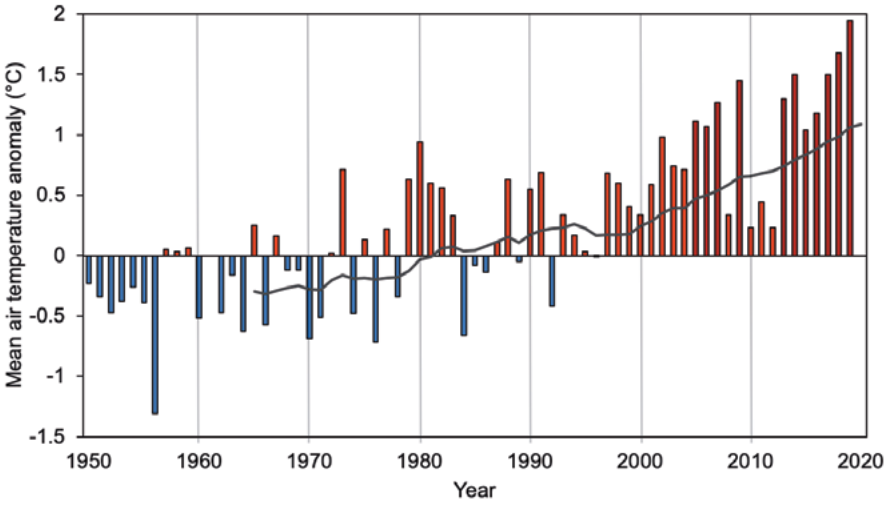

FIGURE 3: Warming in NSW. The graph depicts mean air temperature anomalies (i.e., the deviation of the mean annual air temperature from the long-term (1961-1990) mean). Cooler than average years are shown in blue, warmer than average years in red. The eleven hottest years since 2005 are shown in dark red. The highest ever recorded anomaly is shown for the year 2019. The black line shows the 15-year moving mean. Data was sourced from the Bureau of Meteorology, Commonwealth of Australia.

The long-term trend of increasingly warmer air temperatures in NSW is clear (Fig. 3).

Similar to the state-wide trend, the summer climate of Western Sydney is also heating up. Data from the Bureau of Meteorology show that the number of days where maximum air temperatures are at or above 35°C and especially the number of extremely hot days (at or greater than 40°C) are becoming more frequent. This information can be refined to illustrate that the number of these hot and extreme days is not only increasing in the peak or summer when schools are closed for holidays but is also increasing when schools are open (Fig. 4). Especially the number of days with extreme temperatures during summer school time has tripled from the 1970s to the 2010s (see black trend line in Fig. 4B).

Over the past 40 years, the mean maximum temperature during summer school time has increased by 1.3°C with a clear upward trajectory. The mean maximum temperature for the summers between 2010 and 2020 was as high as those measured for peak summer in the 1990s. Based on these trends and the predicted climate changes for southeast Australia, children will be exposed to increasing heat during summer when schools are open. These climate observations also underline the relevance of the present research that took place during the summer holidays, as it provides an outlook to summer conditions schools will have to deal with in the near future.

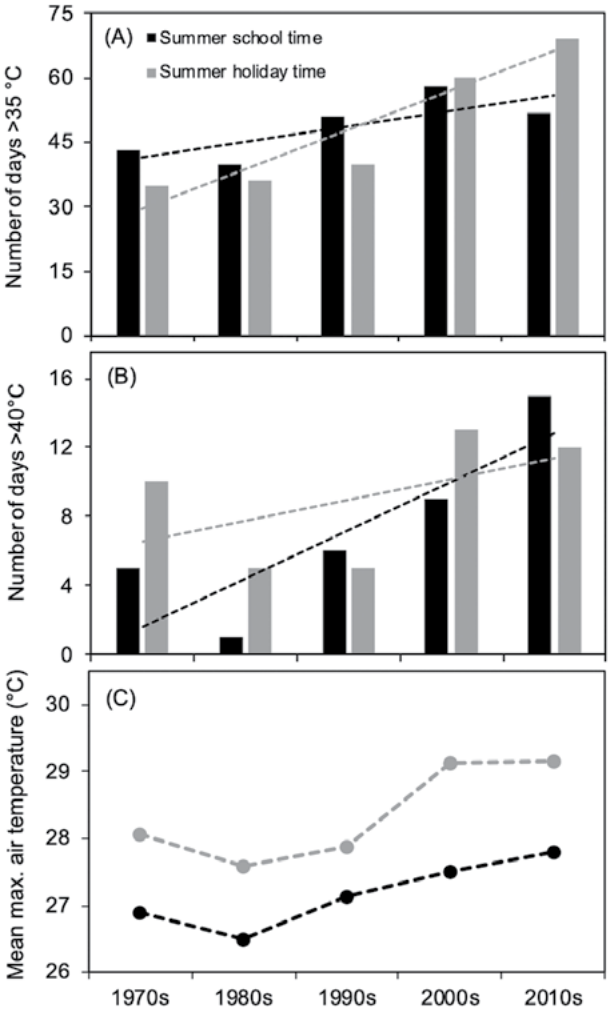

FIGURE 4: Trends of summer heat over the past 50 years during and outside of school times in Western Sydney. Data covering the intervals from 20 November to 20 December and 1 to 28 or 29 of February were used to represent summer school time; data covering the days from 21 December to 31 January were used to represent summer holiday time. Panel A depicts the number of days per decade where air temperatures were at or greater than 35°C. Panel B shows the same type of information for days at or above 40°C. Panel C shows the mean maximum temperature for the past five decades. Data from the Bureau of Meteorology's official weather station #066124 was used for the calculation.

Schools will have to find solutions to deal with increasing heat today. But design and building guidelines or handbooks that assist landscape architects, designers, infrastructure planners, school managers and principals to create cool, thermally inert, safe outdoor environments in schools are missing. However, to maintain outdoor activities and promote the positive physical and mental development of children, it is imperative that such guidelines are developed and used to support the construction of thermally resilient school environments.

Lowering outdoor temperature in school environments is far more difficult to achieve than cooling classrooms. School infrastructure is often dominated by hard, impervious materials for surfaces and buildings that can absorb and radiate large amounts of solar energy (Ma et al., 2017). In contrast, pervious surfaces and vegetation can provide cooling through shade and evapotranspiration, and a number of design elements are available to increase cooling in school yards.

One of the most effective cooling strategies to reduce heat in school outdoor environments is to increase tree cover and associated canopy area (Antoniadis et al., 2016). The cooling effect of trees has been described in countless studies and is provided through shading of surfaces and evaporative cooling. Shading reduces the absorption and radiation of solar energy by surface materials. Especially a reduction of long-wave infrared radiation reduces the flux of sensible heat from the shaded materials. While this effect is confined to the local area of shade projected by the tree canopy, the effect of evaporative cooling reaches further. During the process of transpiration, solar energy is converted to biochemical energy, which contributes to latent heat flux cooling. The air around leaves is cooled and blown into the surrounding space by air movement. This effect leads to lower air temperatures commonly observed under individual trees, in and around urban parks and along urban-rural gradients (Norton et al. 2015; Koc et al., 2018; Pfautsch and Rouillard, 2019A).

Given the high – and for a rising number of days, extreme – risk from heat for immediate wellbeing and long-term development of children, it is timely and sensible to address issues related to heat now. How can heat be mitigated in schools, inside and outside? What are the best materials, shade structures and sustainable technologies to build cooler school yards and retrofit those we already have?

This report provides a starting point to understand school outdoor microclimate. It explains the contribution of common surface materials to sensible heat. It explores the capacity of shade to deliver cooling. Most importantly, it provides practical, evidence-based recommendations how to improve heat resilience of school infrastructure and thus how to make schools safer and more enjoyable for children and teachers. Only the combined efforts of providing optimal learning conditions inside classrooms and creating thermally resilient outdoor environments will result in genuine heat-smart schools.

2. AIMS

This project is part of the Cool Schools Initiative of Western Sydney University. It documents the microclimate around an existing public school in the geographic centre of Greater Sydney. Variation of air and 'feels like' temperature across numerous locations of the school is analysed. Further, this study links microclimates with build and green infrastructure as well as surface materials to inform strategies to mitigate heat in school environments of NSW. This report aims to assist principals, managers and teachers to increase resilience and health of school children during increasingly hot summers and provide planners and architects with options that can improve the thermal performance of new and existing school infrastructure.

3. METHODOLOGY

3.1 SITE DESCRIPTION

Data for this study were collected during the summer break 2019/2020 at a public primary school in Western Sydney, NSW. The school was built in 1949 and covers a total area of approximately 18,000 m^2. The school grounds are situated on a gentle north-south slope with a concentration of buildings in the north and central section and mostly green, open space in the south. Generally, the area covered by the school can be separated into three coarse categories: (1) buildings (27%), (2) other hard, impervious surfaces (32%) and (3) open space (41%).

BUILD ENVIRONMENT

Building stock at the school consists of a range of typologies. Nine single-storey brick buildings and two buildings with walls made of corrugated iron sheets represent the 'permanent building stock'. These buildings provide space for administrative offices, the library, communal hall and classrooms. In addition, one large covered outdoor learning area (COLA, 513 $m^{2)}$ is located to the north-east of the central school yard, and a smaller COLA (132 $m^{2)}$ can be found integrated between permanent buildings to the north of the school.

Based on roof area, these buildings cover 3,100 $m^{2.}$

Between 2008 and 2018, the number of students at the school doubled from 269 in 2008 to 529 in 2018. To mitigate the resulting pressure on classroom space, a number of semi-permanent classrooms were installed at the school. At the time of this study, 21 semi-permanent classrooms were operated at the school, covering approximately 1,785 m^2 (Fig 5). Except for the administration building, which has a dark grey roof made from cement shingles, all permanent and semi-permanent buildings and pergolas have light-coloured roofs made from corrugated iron. Based on roof area, all permanent and semi-permanent buildings, together with a new toilet block cover 4,930 (27%) of the school grounds.

Hard surfaces around the school include a carpark, driveway, concrete and asphalt walking paths, two playgrounds covered in artificial grass and a single large central yard (approx. 2,400 $m^{2)}$ made from asphalt. Pergolas extend to a total length of 225 m,

providing shade to walkways around the school. All pergolas use corrugated iron sheets as roofing material. At least two large rainwater tanks exist at the school. Runoff from roofs is collected in these tanks without immediate use.

OPEN SPACES

The school has nine larger areas of open space, together covering 7,360 m^2. A 'green belt' which includes the majority of tree stock is present along the fenced perimeter of the school. Two large continuous green open spaces exist at the northern and southern end of the school. In the north, a large garden (1,840 m^2) extends from the eastern to the western boundary of the school. This area is dominated by lawn, garden beds and some mature trees. By far the largest open space is found at the southern end of the school, where more than 4,000 m^2 are covered by lawns and trees. During the time of this study, large patches of bare ground were visible, as grass had died back due to drought, heat and outdoor activities prior to summer holidays.

SHADE

Shaded areas at the school were limited. More than 70% of the central school yard was unshaded black asphalt. A mature White Mahogany (*Eucalyptus acmenoides*) tree with a crown diameter of 22 m provided around 400 m^2 shade on buildings, walkways and the school yard. A shade sail (100 m^2) shaded the playground in the eastern section of the central school yard. A range of trees provided shade for buildings along the eastern and western fence line and throughout the large open space in the south. A detailed analysis of shade area provided by trees is provided later in the report. In addition, pergolas and COLAs shaded concrete and asphalt surfaces.

FIGURE 5: Aerial view of the school grounds on (A) 14 November 2009 and (B) 21 January 2020. The yellow line depicts the outer perimeter of the school grounds. In 2009, work for the new school hall commenced. Losses of open space and tree canopy between 2009 and 2019 are clearly visible along the northern boundary, central section and southern open space of the school. Image© Nearmap.

3.2 **DATA COLLECTION**

A range of measurements were collected in this project. A list of measured and remotely assessed parameters, time of collection and units are shown in Table 1.

TABLE 1: Type, time and units of measurements collected for this study.

MEASUREMENT	MODE OF RECORDING	TIME OF COLLECTION	UNIT
Tree canopy cover	remotely	01 February 2020	m^2
Tree inventory and health	once	23 January 2020	N/A
Air temperature	permanent	16 December 2019 – 26 January 2020	°C
Air temperature Black globe temperature Surface temperature (on ground)	periodic	19 December 2019 30 December 2019 14 January 2020	°C
Surface temperature (drone-based)	periodic	23 January 2020 27 January 2020	°C
Relative humidity	permanent	19 December 2019 – 26 January 2020	%
Tree water use	permanent	21 December 2019 – 26 January 2020	$L\ h^{-1}$

Data were collected from a large number of locations, covering the entire school outdoor environment, all major ground surface types (grass, bare soil, asphalt, concrete, artificial grass), sunlit and shaded locations, COLAs, pergolas and tree groves (Fig. 6).

FIGURE 6: Location of permanent air temperature monitoring stations (red dots, n = 20), periodic measurements of 'feels like' temperatures in the sun (white triangle, n = 4) and the shade (grey triangle, n = 4) and tree water use measurements (blue diamonds, n = 10). The TinyTag sensor housed in the Stephenson Shield is depicted as yellow square. White scale bar is 50 m. Image© Nearmap.

3.2.1 TREE INVENTORY AND CANOPY COVER

A detailed tree inventory for the school was completed in January 2020. For the inventory species, stem diameter (at 1 m aboveground), total and canopy height of all trees and tall shrubs were recorded. In addition, information about the physical appearance of each tree, such as single or multi-stemmed character and health was assessed. For the health assessment, a visual technique was used that scores the presence or absence of foliage and dead branches (Fig. 7). The social status of all trees was dominant, and no tree hollows were present at the site. Canopy cover of trees and tall shrubs was quantified using high resolution aerial images from February 2020 (Nearmap, Sydney, Australia).

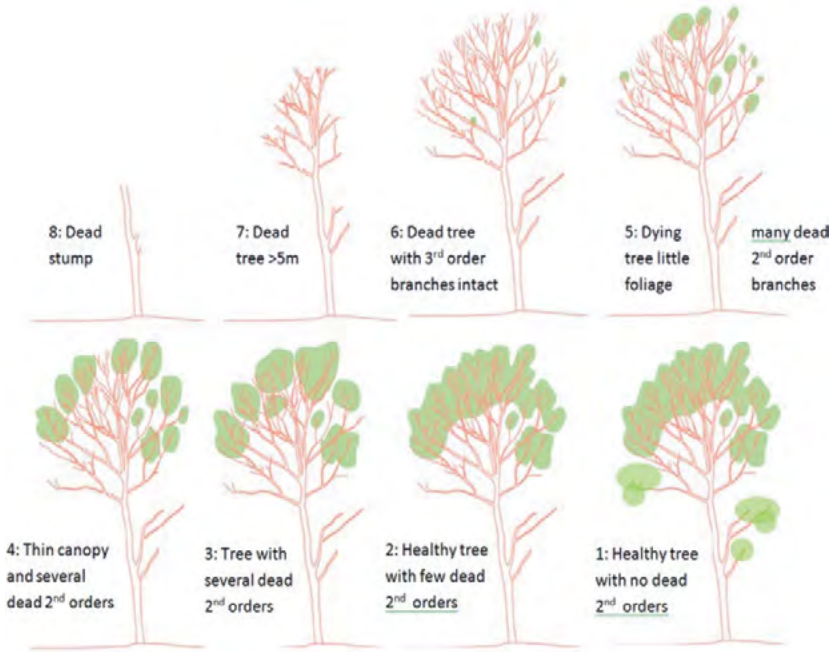

FIGURE 7: Scoring system for the visual assessment of tree health. Courtesy of Macquarie University.

3.2.2 AIR TEMPERATURE

Two different devices were used to permanently record near surface air temperature (i.e. 2-2.5 m above ground). The first device was designed by Western Sydney University and consisted of a single-use temperature sensor with integrated logger. The high accuracy (±0.5°C (-20°C/+40°C)) and resolution (0.1°C) of the sensor (Tempmate®-S1 V2, Imtec Messtechnik, Heilbronn, Germany) has been certified by international standards (e.g., CE, EN 12830). The sensor was enclosed in a waterproof plastic casing and programmed to record air temperature (T_{air}) at 10-minute intervals from 17 December 2019 to 26 January 2020 (41 days). The sensor was positioned inside a protective shield to prevent exposure to direct solar radiation. The high-gloss white colour together with the open base and holes in the top of the protective shield prevented heat to build up around the sensor (Fig. 8). From here on, the combination of sensor and its protective shield will be referred to as a *heat logger.*

Accuracy of the heat logger was validated against three official weather stations from the Commonwealth Bureau of Meteorology and a commercially available sensor (Pfautsch and Rouillard, 2019B). All calibrations yielded high coefficients of determination, indicating that the heat logger was capable of accurately recording air temperature. Twenty heat loggers were distributed across the school grounds (Fig. 8), where they were mounted on tree branches, under walkways, in green spaces, the main playground and the carpark. Sunlit, partial- and fully-shaded locations were selected to represent broad site characteristics and spatial coverage of the school grounds (see red dots in Fig. 6). Performance of heat loggers under similar conditions in previous projects indicated no impact of direct solar radiation on temperature measurements. All 20 heat loggers were retrieved at the end of the measurement period, yielding 118,080 individual measurements for analysis.

FIGURE 8: Image of the two devices used for collection of permanent air temperature information. (A) Mounting the Tempmate® sensor into the protective shield. (B-E) Heat logger at several locations across the school (red diamonds A, C, F and L in Fig. 5). (F) Stephenson screen containing a TinyTag logger (yellow square in Fig. 5). Image© S. Pfautsch.

The second device was a commercially available temperature and relative humidity sensor (TinyTag TPG-4500, Hastings Dataloggers, Port Macquarie, Australia) housed inside a Stevenson Shield (ACS-5050, Hastings Dataloggers). The shield was hung from the branch of a mature Queensland Brush Box (*Lophostemon confertus*) tree in the teacher's carpark and set to record data at 15-minute intervals (Fig. 6). At the end of the measurement period the TinyTag logger had recorded 7,392 individual measurements.

3.2.3 MICROCLIMATE MAPS

Permanent measurements of T_{air} were used to develop the first geo-referenced, microclimate heat maps for a school environment in Australia. For this purpose, the 20 geographic locations of heat loggers were recorded, and location-specific data were imported into ArcGIS 10.6 to create shapefiles based on GPS coordinates. Inverse Distance Weighted (IDW) interpolation was used to estimate continuous raster temperature maps from temperature values recorded at the location of each heat logger. The resulting temperature value of each pixel in raster maps was estimated according to values of the 12 nearest locations in the shapefile. The influence of each location on the temperature value of each pixel declined with distance to the pixel. Raster maps produced from IDW interpolations were clipped at the boundary of the school. Finally, to display air temperature variation it was necessary to optimise a graduated colour scheme for each map. Each shade of the gradual changes represents a fixed temperature value interval, which is specified in the caption of the map.

The following map types were produced:

- *Overview map* – showing the mean temperature environment across the school for the duration of the project and at distinct 2-hour time intervals during the operational hours of the school (8:00-16:00)
- *Process map* – depicts how quickly temperatures increase between 6:00 and 10:00
- *Focus maps* – providing a visualisation of T_{air} during time intervals of the morning recess and lunch break; a graphical representation of Tair during the peak of the heatwave event on 4 January 2020.

3.2.4 THERMAL COMFORT

As an approximation for human thermal comfort, we calculated a Heat Index (HI) based on measurements of T_{air} and relative humidity following equations from the National Oceanic and Atmospheric Administration (NOAA) of the United States (https://www.wpc.ncep.noaa.gov/html/heatindex_equation.shtml). The HI represents a simple measure of 'feels like' temperature and is separated into four risk levels (Table 2).

TABLE 2: Heat Index Guidelines from the National Oceanic and Atmospheric Administration (NOAA) of the United States.

HEAT INDEX	RISK LEVEL	PROTECTIVE MEASURES
Less than 32.8°C	Lower (Caution)	- Basic heat safety and planning
32.8 – 39.4°C	Moderate	- Drink 1 L of water per hour - Take breaks when needed
39.4 – 46.1°C	High	- Drink water every 15-20 minutes - Take frequent breaks - Alert personnel of high heat risk of the day
Greater than 46.1°C	Very High to Extreme	- Drink water frequently - Alert personnel of extreme heat risk for the day

The HI was calculated for each of the 20 measurement locations, using location-specific temperature data and measurements of relative humidity from the TinyTag logger located in the teacher's carpark. The data recorded at the teacher's carpark represented the closest and continuous record of this parameter, however, we acknowledge that relative humidity could have varied among the 20 locations. For each location we calculated the HI and identified the risk level on an hourly bases for the time interval between 8:00 and 16:00 (operational hours of the school) from 20 December 2019 to 26 January 2020.

In addition to the assessment of thermal comfort at the 20 measurement locations, we collected spot measurements of $T_{air,}$ black globe temperature (T_{bg}) and HI using portable micro-meteorological stations (Model 5400, Kestrel Instruments, Boothwyn, United States). The stations were mounted on tripods and were programmed to record data at 30-second intervals.

While the HI is a simple representation of a 'feels like' temperature based on T_{air} and relative humidity, we included measurements of T_{bg} in the study, because they represent a more complex 'feels like' temperature that incorporates radiated energy from the ground and cooling by wind.

The black globe thermometer was designed to measure temperature as felt by a human body when seated. The micro-meteorological stations recorded T_{bg} inside a 1-inch (2.54 cm) diameter copper, matt black sphere. T_{bg} represented a composite measurement of air temperature, wind speed, heat transfer by incident solar radiation and convection of heat between the globe and the environment (Oliveria, 2019).

The micro-meteorological stations were used to record T_{air} and T_{bg} and HI at each of five paired (sunlit and shaded) locations that had identical surface characteristics (Fig. 9). The five locations are marked with triangles in Figure 6. Location 1 was on lawn in the front garden, location 2 on asphalt in the main school yard, location 3 on artificial grass at the playground, location 4 on the concrete walkway between two rows of semi-permanent classrooms and location 5 on bare soil in the southern open space.

To calculate a representative mean value for each parameter and location and light condition (sunlit, partial- and full-shade), 10 sequential 30-second measurements were averaged at the end of a 15-minute recording interval. Measurements were collected between 12:00 and 15:00 on three days of summer (19 December 2019, 30 December 2019, 14 January 2020).

FIGURE 9: Recording of black globe temperatures (TBG) using the micrometeorological weather station. (A) Central school yard on asphalt in full sun. (B) At the entrance of the communal hall on concrete in the shade. (C) Tree grove at the western fence on dry grass and leaves in the shade. Image© L. Vu.

3.2.5 SURFACE TEMPERATURE

Surface temperatures were measured using an infrared camera (T540, FLIR Systems, Wilsonville, United States). All major surface types, sunlit and shaded, throughout the school were imaged at the same time as when T_{bg} and T_{air} were recorded, resulting in a total of 302 high-resolution thermal images used for analysis of surface temperatures (Fig. 10).

The FLIR Tools software was used to extract more than 900 individual temperature measurements from images. For each surface type, at least nine individual measurements were averaged. The surface types that dominated the premises were measured in pairs of sun/shade and included asphalt, artificial grass, concrete, bare soil and dry grass. Surface temperatures were also assessed for green vegetation, including lawn, shrubs and tree canopy. Additional infrared images were used to analyse surface temperatures of building walls made from brick (old building stock), cement sheets (semi-permanent classrooms) and sheet metal (old building stock).

For the assessment of surface temperatures of roofing materials and to allow simultaneous measurements of across the entire school, we use a drone with thermal imaging capacity (Fig. 11). The drone (M210 RTK, DJI, Shenzen, China) and dual-mode camera (XT2, FLIR Systems) was flown at 80 m elevation within the boundaries of the school.

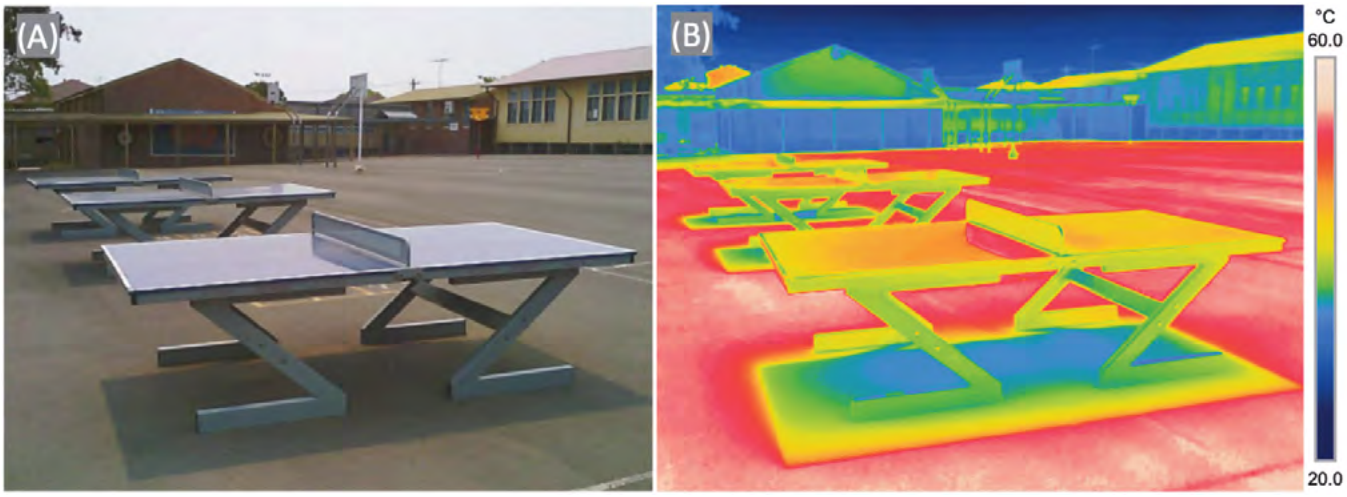

FIGURE 10: Example of a normal view and infrared view of the ping-pong tables in the central school yard. The image was taken during the afternoon in full sunshine (30 December 2019). Surface temperatures of the tables was 48.5°C, asphalt in the sun was up to 56°C, while in the shade underneath the tables around 37°C, highlighting the pronounced cooling effect of shade on dark surfaces (a difference of 19°C). Image© S. Pfautsch.

FIGURE 11: Matrice 210 RTK drone with FLIR XT2 camera for aerial assessment of surface temperatures. Image © D. Pataki.

The energy associated with electromagnetic radiation from the sun is either reflected, absorbed, transmitted or refracted when it hits a surface. The proportion of energy that is attributed to each of the four processes depends on the characteristics of the material as well as its exposure and orientation to the incoming radiation. This is clearly a simplification of the physical processes involved when objects of a given thermal mass heat up. However, being aware of these characteristics and processes will be helpful to understand the origin of higher or lower surface temperatures of the materials assessed across the school outdoor environment. As a rule of thumb, materials with low reflectance, high absorption, zero transmission or refraction, with a large thermal mass and full exposure to sunlight will display high surface temperatures and reradiate large proportions of absorbed energy as sensible heat.

3.2.6 TREE WATER USE

Water use of 10 trees was measured during December 2019 and January 2020 using a heat pulse method (Table 3). This required implanting sensors (HPV-o6, Edaphic Scientific Pty Ltd, Melbourne, Australia) into the water conducting wood (i.e., sapwood) of tree stems (Fig. 12 A). Once the sensor head containing three probes (Fig. 12 B) was positioned and the equipment was activated, the central heater probe system released a heat pulse every 15 minutes. Probes above and below the heater recorded the temperature change following the release of the pulse for a fixed period of time. The change in temperature difference between the probes was used to estimate the velocity of the heat pulse.

TABLE 3: Physical characteristics of trees for water use measurements. 'ID' indicates the locations of trees in Fig. 6. Ds = stem diameter at 1 m aboveground; Wb = bark width; θsw = moisture content of sapwood; ρsw = density of sapwood; Dsw = depth of sapwood; Asw = area of sapwood.

ID	SPECIES	COMMON NAME	TREE HEIGHT (M)	D_S (CM)	W_B (CM)
0	*Ulmus parvifolia*	Chinese Elm	12.1	29.1	0.4
1	*Lophostemon confertus*	Queensland Brush Box	12.7	52.3	2.1
2	*Ulmus parvifolia*	Chinese Elm	14.3	38.2	0.7
3	*Corymbia maculata*	Spotted Gum	27.4	45.9	1.7
4	*Ulmus parvifolia*	Chinese Elm	12.2	24.3	0.5
5	*Lophostemon confertus*	Queensland Brush Box	16.5	81.4	2.5
6	*Eucalyptus sp.*	Gum tree	21.6	40.4	1.9
7	*Banksia integrifolia*	Coast Banksia	9.9	28.2	1.5
8	*Allocasuarina sp.*	Sheoak	13.8	24.5	1.5
9	*Glochidion ferdinandi*	Cheese Tree	9.7	57.8	0.9

Conversion of heat velocity data to tree water use (Q in L per hour (L h^{-1})) required knowledge of additional parameters for each tree:

1. Sensor depth – fixed at 8 and 18 mm inside the sapwood
2. Bark width – measured with a bark depth gauge
3. Moisture content, density and depth of conducting sapwood – these were assessed by extracting a fresh wood core (5 mm diameter) using an increment borer (Fig. 12C); depth of conductive sapwood was measured with a digital calliper; weight and volume of a piece of fresh sapwood was determined in the field using a 3-point digital balance; this piece of sapwood was dried at 105°C for 3 days and dry weight determined; moisture content and density was calculated using these measurements
4. Total conductive area of trees – this parameter was estimated using information about bark width, tree diameter and sapwood depth

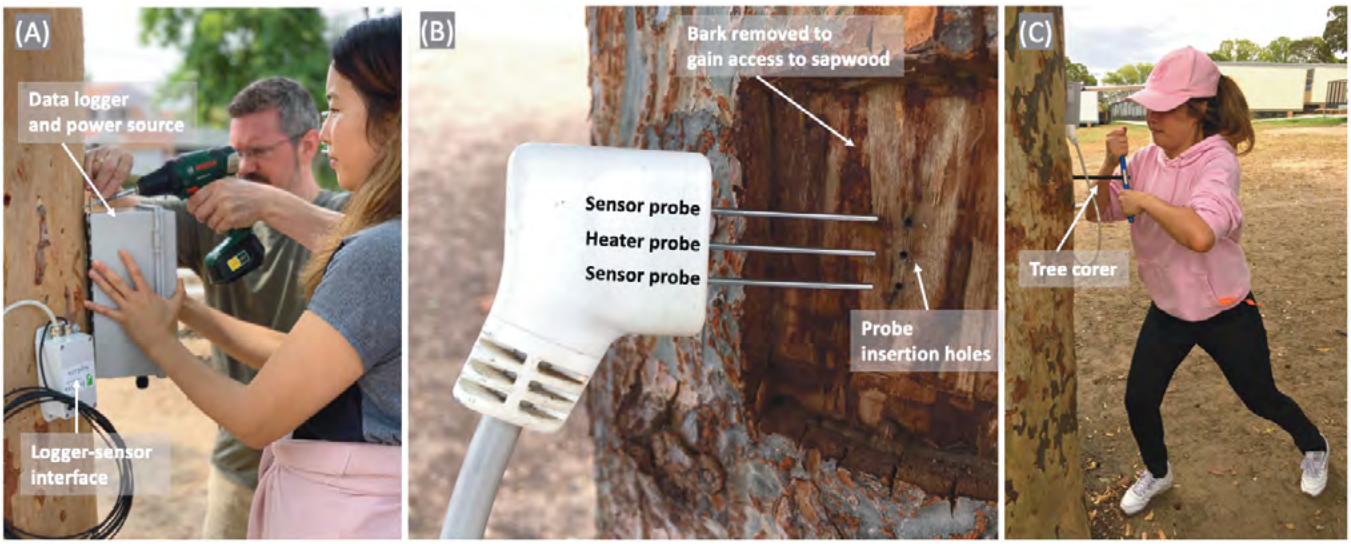

FIGURE 12: Tree water use work at the school. (A) Installation of data loggers and relevant auxiliary equipment. (B) Sensor head with probes before insertion into the stem; probe diameter is 1.25 mm. (C) Extraction of wood core to determine sapwood depth, moisture content and density. (A) Image© L. Vu; (B, C) Image © S. Pfautsch.

The driving force of tree water use is vapour pressure deficit (VPD) of the atmosphere (in kPa). We calculated VPD from measurements of air temperature (T_{air}) and relative humidity (rH) from the TinyTag logger after Snyder and Shaw (1984):

$$VPD = \left(0.6108 \times \left(\frac{\exp\left(17.27 \times T_{air}\right)}{T_{air} + 237.3}\right)\right) \times \left(1 - \frac{rH}{100}\right)$$

3.2.7 TREE SELECTION TOOL

To inform the selection of suitable tree species for planting in schools, we developed the 'Tree Species Finder'. For this tool, the frequency of individual street tree species across central Western Sydney was investigated using data provided by the council. From the 244 species identified in the database we selected the 30 most abundant species for the tool (Table 4).

In a next step, we evaluated seven characteristics that influence the suitability of each species for open spaces around school infrastructure. These characteristics were: (1) branching height when trees are mature (i.e., how good is the tree for climbing), (2) amount of shade provided when mature, (3) if the species is known to drop green limbs, if it is (4) poisonous or (5) produces known allergens, (6) has thorns or spikes, and (7) edible fruit. Each of these factors were then weighted from low to high for each species. In a final step, we defined three different scenarios to demonstrate how the tool selects species according to the importance assigned to each of the seven characteristics (Table 5). Scenario 1 was focussed on multiple safety aspects, scenario 2 was only concerned about limb drop, and scenario 3 was designed to identify 'allrounder' species that provided a range of benefits.

TABLE 4: List of the 30 most abundant street tree species in central Western Sydney in 2019.

SPECIES NAME	COMMON NAME	FREQUENCY
Callistemon viminalis	Weeping Bottlebrush	9194
Lophostemon confertus	Queensland Brush Box	3427
Callistemon citrinus	Crimson Bottlebrush	2295
Tristaniopsis laurina	Water Gum	2209
Melaleuca quinquenervia	Broad-leaved Paperbark	1853
Jacaranda mimosifolia	Jacaranda	1699
Eucalyptus sp.	Gum tree	1112
Lagerstroemia indica	Crepe-myrtle	905
Corymbia maculata	Spotted Gum	761
Prunus cerasifera	Cherry Plum	573
Callistemon salignus	White Bottlebrush	490
Liquidambar styraciflua	Sweetgum	478
Elaeocarpus reticulatus	Blueberry Ash	430
Melaleuca linariifolia	Narrow-leaved Paperbark	415
Photinia glabra	Japanese Photinia	390
Casuarina cunninghamiana	River Sheoak	383
Olea europaea	Olive	336
Eucalyptus tereticornis	Forest Red Gum	325
Leptospermum petersonii	Lemon-scented Teatree	303
Angophora floribunda	Rough-barked Apple	257
Cinnamomum camphora	Camphor Laurel	253
Syzygium smithii	Common Lilly Pilly	248
Eucalyptus microcorys	Tallowood	247
Eucalyptus nicholii	Narrow-leaved Black Peppermint	243
Syzygium floribundum	Weeping Lilly Pilly	230
Triadica sebifera	Chinese Tallow	223
Melaleuca bracteata	Black Teatree	222
Agonis flexuosa	Willow Myrtle	219
Melaleuca syphelioides	Prickly-leafed Paperbark	205
Corymbia citriodora	Lemon-scented Gum	200

TABLE 5: Three scenarios for the selection of tree species to be planted at a hypothetical school. Selected characteristics are weighted from 0 (not important at all) to 1 (extremely important).

	BRANCHING HEIGHT	SHADE AREA	LIMB DROP	POISONOUS	PRODUCES ALLERGENS	THORNS AND SPIKES	EDIBLE FRUIT
Scenario 1	0	1	1	1	1	0	0
Scenario 2	0	0	1	0	0	0	0
Scenario 3	0.6	0.8	0.8	0.5	0.3	0.3	0.2

4. PROJECT FINDINGS

4.1 SCHOOL TREE STOCK

The inventory listed 69 trees belonging to at least 18 genera, including at least four different species of *Eucalyptus* and two species of paperbark. The most frequent species was *Lephostomon confertus* (Queensland Brush Box; n = 15), followed by *Allocasuarina sp.* (Sheoak; n = 9) and Eucalyptus sp. (n = 7). Mean stem diameter and height across all trees was 41 cm and 12 m, indicating a mature aged tree stock. Mean canopy height was 9.2 m.

The largest tree was a eucalypt (White Mahogany, *Eucalyptus acmenoides*) with a diameter of 128 cm and a height of nearly 20 m, located at the south west corner of the central school yard. The tallest tree (27.4 m) was a Spotted Gum located near the south eastern fence line. Of the 69 trees, 19 were multi-stemmed. Tree health was generally found to be good or very good, with 53 trees scoring '1' (healthy tree with no dead 2° orders; Fig. 7) and 11 scoring '2' (healthy tree with no few 2° orders), representing 93% of the tree stock at the school. Queensland Brush Box, Cheese Tree and Chinese Elm represented the three most healthy species with a score of 1 for all individuals, representing one third of all trees. One Sheoak was dead (score of 8) and another Sheoak and a Cherry Tree were in serious decline (score of 5).

The shade assessment identified 19 individual tree canopies, 11 canopy clusters and eight tall shrubs providing shade to a total area of 3,677 m^2 (Fig. 12). Individual trees represented a canopy area of 1,360 m^2 (37%). Tree clusters with interlocked canopies covered another 2,103 m^2 (57%), and tall shrubs the remaining 214 m^2 (6%). The large open space at the southern end of the school had a canopy cover of approximately 30% or 1,238 m^2.

The largest single shade area was 551 m^2, provided by a group of mature Queensland Brush Box at the eastern fence line (marked '64-69' in Fig. 13). A large White Mahogany located at the south west corner of the central school yard had the largest canopy area (398 m^2) of any individual tree.

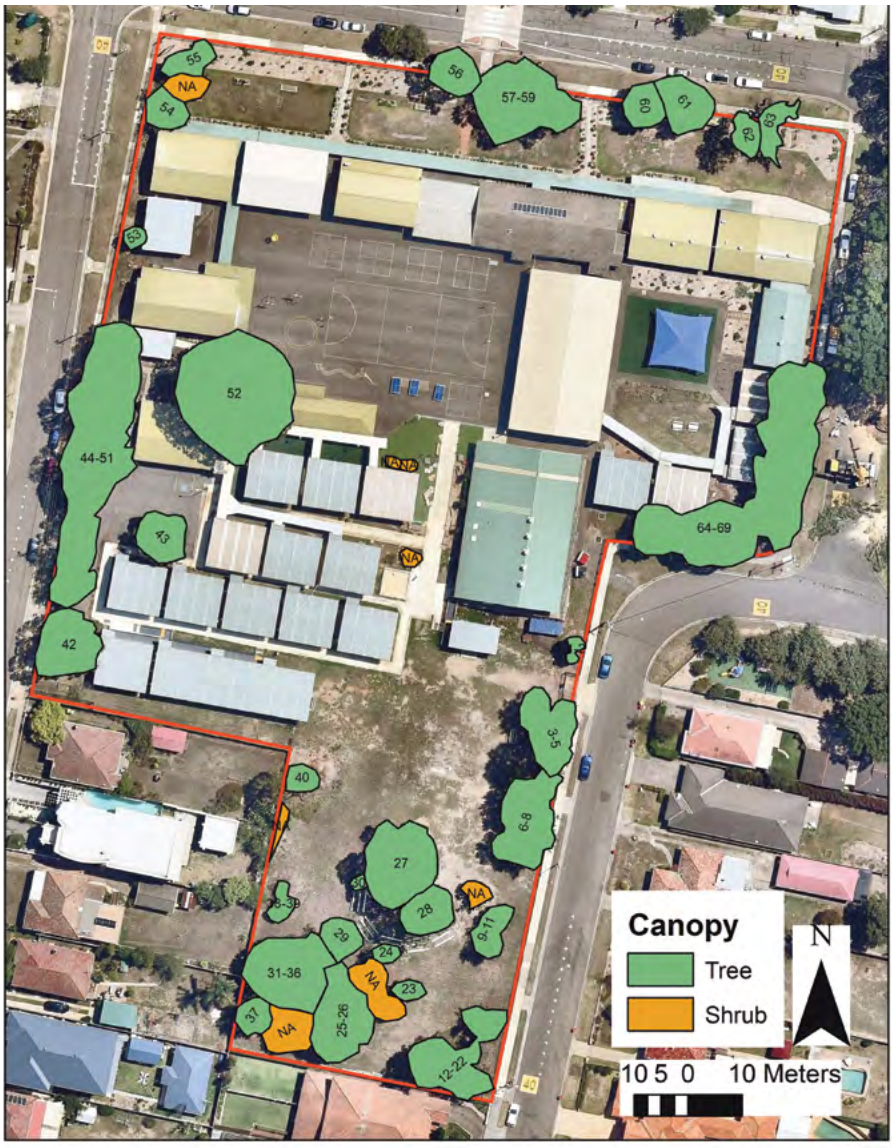

FIGURE 13: Mapped tree canopy cover across the school (January 2020).

Tree shade was missing for the majority of the central school yard, and all semi-permanent classrooms in the south, leading to absorption of large quantities of solar radiation and radiation of absorbed energy as sensible heat. Large gaps of trees existed along the north western and northern fence line, leaving administration buildings, the library and several classrooms exposed to direct solar radiation during most of the day. The pergola in front of these buildings did reduce direct sunshine into the north-facing windows, however, the absence of tree shade left the front of the school exposed to heat.

4.2 THERMAL ENVIRONMENT

4.2.1 PATTERNS IN AIR TEMPERATURE

Weather conditions during the project were generally hot and dry. During the 41 days of the project, heat loggers located across the school recorded 18 days where maximum T_{air} was greater than 35°C (defined as 'hot days' by the Bureau of Meteorology) and 8 days where maximum Tair was more than 40°C (defined as 'extreme days' by the Bureau of Meteorology). Across the school, mean T_{air} during the project was 24.6°C and mean maximum and mean minimum T_{air} of 25.9°C and 23.5°C, respectively. The hot zone of the school was in the north east and the cool zone in the south (Fig. 14).

The location of hot and cool zones across the school matched well with areas that heated up more or less quickly during morning hours (Fig. 15). To assess rates of mean warming, the difference of T_{air} between 6:00 and 10:00 was calculated for each of the 20 heat logger locations. During this time interval, the morning sun warmed up T_{air}, surfaces and structures more or less quickly depending on convection and air flows, as well as thermal properties of materials and their degree of being under shade. Locations where trees provided shade warmed only 6.5-7.5°C slowly (locations A, H, J, K, M, P, Q, S, R in Fig. 6), while T_{air} rose on average 8.5-9.5°C at locations that were entirely without shade (e.g. locations E, F, O in Fig. 6). Air temperatures increased the most – by 10.0-11.0°C - where shade was provided by corrugated iron (e.g. locations C, D, L in Fig. 6) or dark shade cloth (location G in Fig. 6).

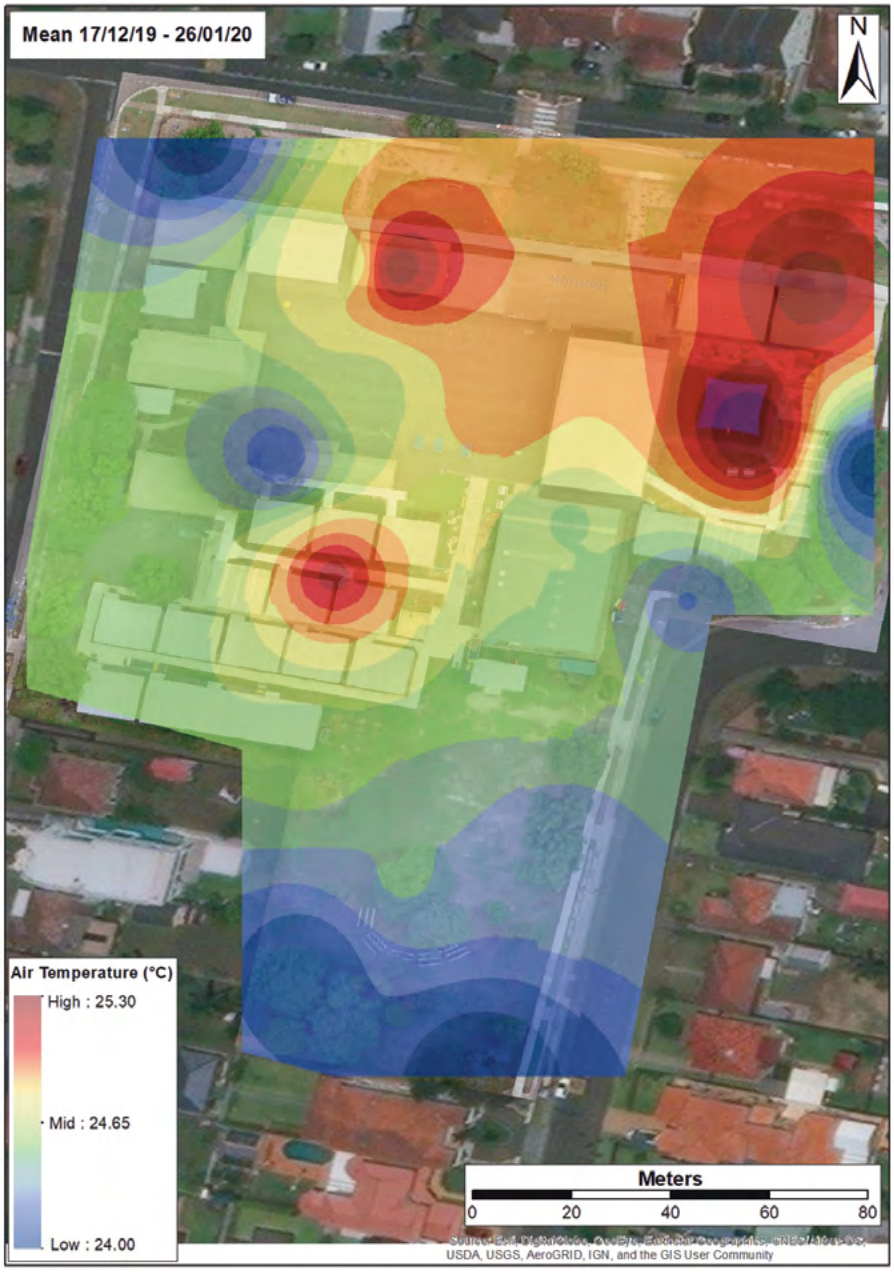

FIGURE 14: Interpolated mean air temperatures across the school using all available data between 17 December 2019 and 26 January 2020.

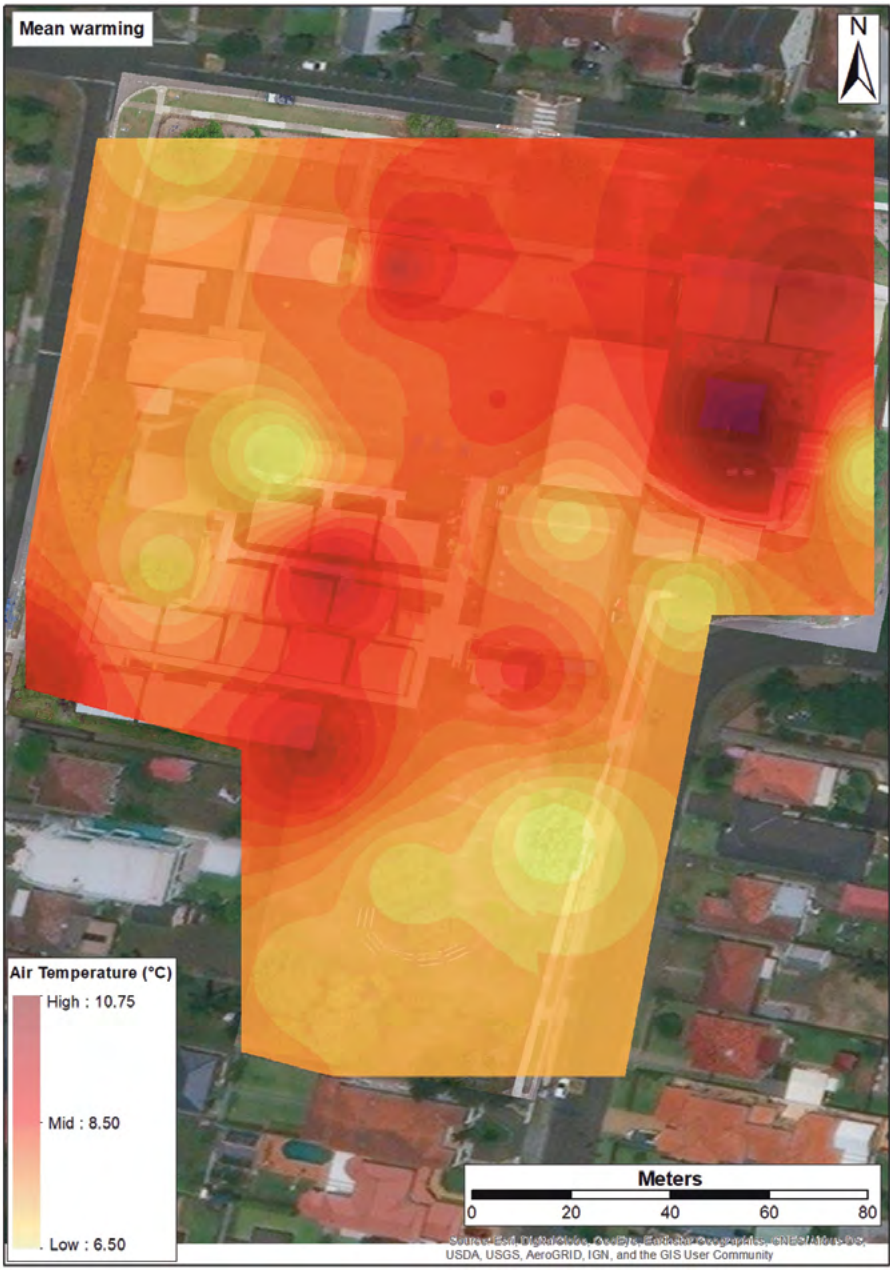

FIGURE 15: Mean warming of air temperature calculated as difference between 6:00 and 10:00. Data spanning 17 December 2019 and 26 January 2020 were used for the calculation.

Mean T_{air} was generally cooler under trees compared to open spaces without trees and built environment (Table 6). When averaged across the 41 days, the coolest environment was at the south-eastern corner of the school grounds (position R in Fig. 6) where mean T_{air} was 24.0°C. The hottest environment was located at the playground where mean T_{air} was 25.3°C (position G in Fig. 6). As mentioned above, the hottest individual temperature was measured at the playground. The coolest individual temperature was 13.6°C, measured in the early morning hours (04:40 and 04:50) of 17 December 2019 at the open space along the south west fence line (positions O and T in Fig. 6).

TABLE 6: Mean air temperature (T_{air}) measured between 17 December 2019 and 26 January 2020 for all 20 locations of heat loggers across the school. Locations are listed from coolest to warmest mean T_{air}. Location ID matches with red dots shown in Fig. 5. For each location n = 5904.

LOCATION ID	T_{AIR} (°C)	SITE CHARACTERISTIC	LIGHT ENVIRONMENT
G	25.3	Playground area	Shade
C	25.2	Assembly area	Shade
D	25.2	Pergola in front of library	Shade
L	25.0	Pergola between semi-permanent classrooms	Shade
F	24.9	Central school yard (east)	Sun
B	24.7	Passageway between buildings	Shade/sun
E	24.6	Central schoolyard (west)	Sun
I	24.6	Front area of Assembly Hall	Shade
T	24.6	Open space near driveway	Sun
O	24.6	Open space at semi-permanent classroom	Shade/sun
N	24.6	Open space at toilet block	Shade/sun
K	24.5	*Lophostemon* tree	Shade
Q	24.5	*Lophostemon* tree	Shade
P	24.4	Row of *Ulmus* trees	Shade/sun
M	24.4	Grove of *Lophostemon* trees	Shade
H	24.3	Under pergola	Shade
S	24.2	Grove of *Glochidion* trees	Shade
A	24.1	*Lagerstroemia* shrub	Shade/sun
J	24.1	Grove of *Lophostemon* trees	Shade
R	24.0	Grove of *Casuarina* trees	Shade/sun

When comparing locations that were completely shaded with those where shade was absent, it became clear that direct exposure of heat loggers to solar radiation did not lead to higher temperature readings. For example, microclimate of the playground area (fully shaded, position G in Fig. 6) was always warmer compared to that of the central school yard (no shade, position E in Fig. 6). Differences in T_{air} were most pronounced during midday where T_{air} at the playground could be 6°C higher compared to other locations of the school's outdoor spaces (Fig. 16). These temperature differences originated from a range of compounding factors.

The dark shade cloth above the playground caused air to heat up and become trapped under the shade structure. Absorbed and radiated heat from artificial grass around the unshaded section of the playground further increased the local heat load. Lastly, the enclosed, courtyard-like setting surrounding the playground reduced air flows, thereby limiting convection of hot air and its replacement with cooler air. In comparison, air flows were not obstructed in the central school yard and sensible heat could dissipate freely, leading to cooler T_{air}. However, the large thermal mass of the black asphalt resulted in continued radiation of stored heat into the night, leaving T_{air} at night warmer in the school yard compared to the playground (Fig. 16).

Across the Greater Sydney Basin, 04 January 2020 was the hottest day since official temperature recordings commenced at the end of the 19th century. The extreme conditions of the day resulted in mean T_{air} of 47.7°C (±1.6, one standard deviation of the mean) at 13:20 across all 20 positions monitored by heat loggers. Air temperatures of more than 50°C were measured at four independent positions at that point in time (locations D, G, L, T in Fig. 6). The highest T_{air} was 50.5°C, measured at the playground (position G in Fig. 6), the lowest was 45.0°C measured at the front of the assembly hall (position I in Fig. 5) (Fig. 17). The close proximity of the two positions where a difference of 5.5°C was measured at the exact same timepoint underlines the importance of assessing environmental conditions at the micro-scale.

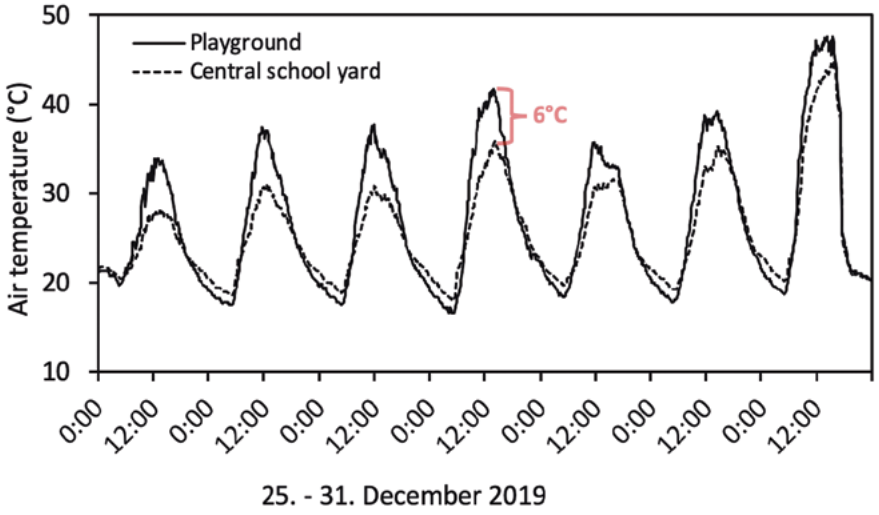

FIGURE 16: Continuous air temperature measurements at the end of December 2019 in a shaded (playground) and a sunlit location (central school yard).

FIGURE 17: Interpolated mean air temperatures across the school during the peak of an extreme heatwave event on 4 January 2020.

4.2.2 AIR TEMPERATURE DURING OPERATING HOURS

Although the school was closed during the project, T_{air} for the time during school operating hours (08:00-16:00) was calculated (n = 2,009 measurements for each location) to assess the temperature environment when students and staff would be on site. Mean T_{air} during operating hours was 28.7°C (± 6.1). After calculating daily mean T_{air} during operating hours for each location, it was found that T_{air} across the school was above 35°C on 6 days and above 40°C on 2 days (Fig. 18), indicating that the entire outdoor space of the school was subjected to enormous heat for the entire time of (theoretical) operation. The largest difference between T_{air} of two measurement locations for the 8-hour interval was 6.0°C, recorded on 28 December 2019 at the playground (hot) and amongst trees on the eastern fence. Notably, large temperature differences were not only evident during days of hot or extremely hot days, but also during days where mean T_{air} was below 30°C (Fig. 18).

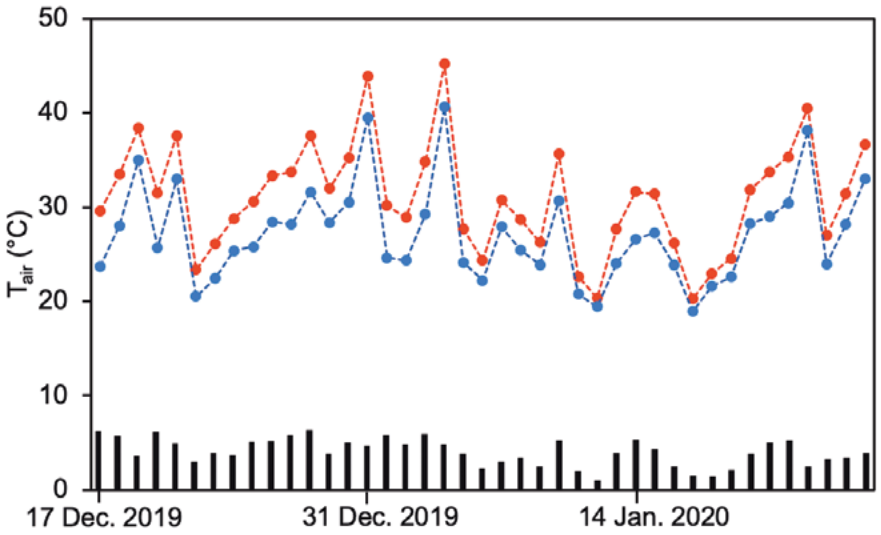

FIGURE 18: Mean air temperature during operating hours (8:00-16:00). Red symbols show the highest mean temperature, blue symbols the lowest mean temperature recorded over the 8-hour interval; black bars indicate the difference between the highest and lowest mean temperatures.

The observed trends for generally hot and generally cool locations remain when calculating mean T_{air} during operational hours for the 41 days of the project. Between 8:00 and 16:00 the playground area had a mean T_{air} of 30.9°C (± 6.0). In contrast, mean T_{air} for the same time span in the *Lephostomon* tree grove near the eastern fence was 27.3°C (± 5.0), representing -1.4°C cooling compared to the school mean and -3.6°C cooling compared to the playground. Across all 20 locations, T_{air} varied, on average, by 4.2°C (± 1.9) during operating hours. The largest absolute difference in T_{air} was recorded during the afternoon of 26 January where a rapid cool change resulted in variation of up to 11.4°C between the south-western (23.3°C; location T in Fig. 6) and north-eastern corner (34.7°C; location D in Fig. 6) of the school.

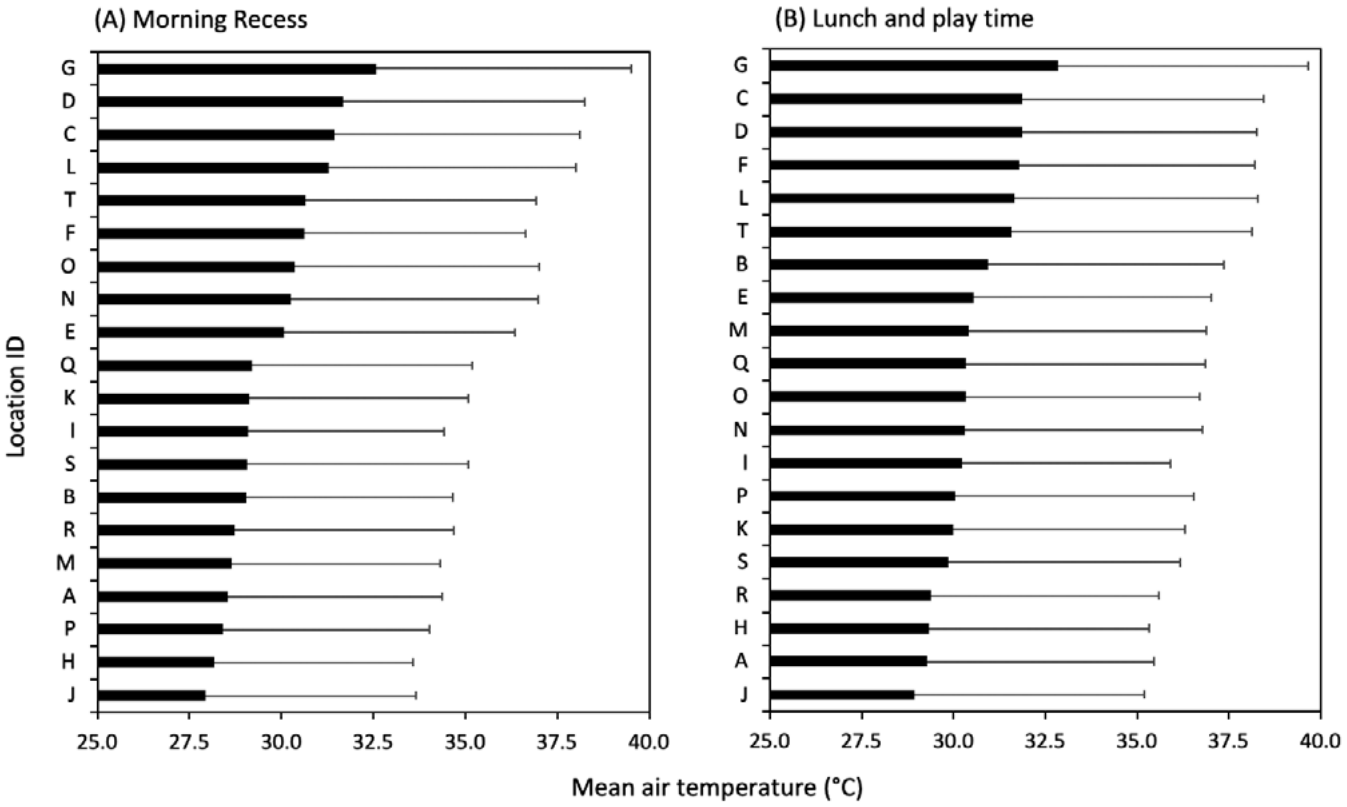

4.2.3 AIR TEMPERATURE DURING RECESS TIMES

Detailed analyses of T_{air} during morning recess (11:10-11:40) and the lunch break (13:20-14:10) were also done. Air temperature varied, on average, by 4.7°C during morning recess and 4.0°C during the lunch break. During both time intervals, the playground area had the highest mean T_{air} and the grove of *Lephostomon* trees near the eastern fence had the lowest mean T_{air} (Fig. 19). The highest single temperature measurement during morning recess was 47.3°C, recorded under the pergola near the library in the north-eastern corner (location D in Fig. 6).

FIGURE 19: Ranking of mean air temperature at the 20 measurement locations across the school – from warmest to coolest during (A) morning recess and (B) lunch and play break. Error bars show 1 standard deviation of the mean. See Figure 6 and Table 6 for details of the Location ID.

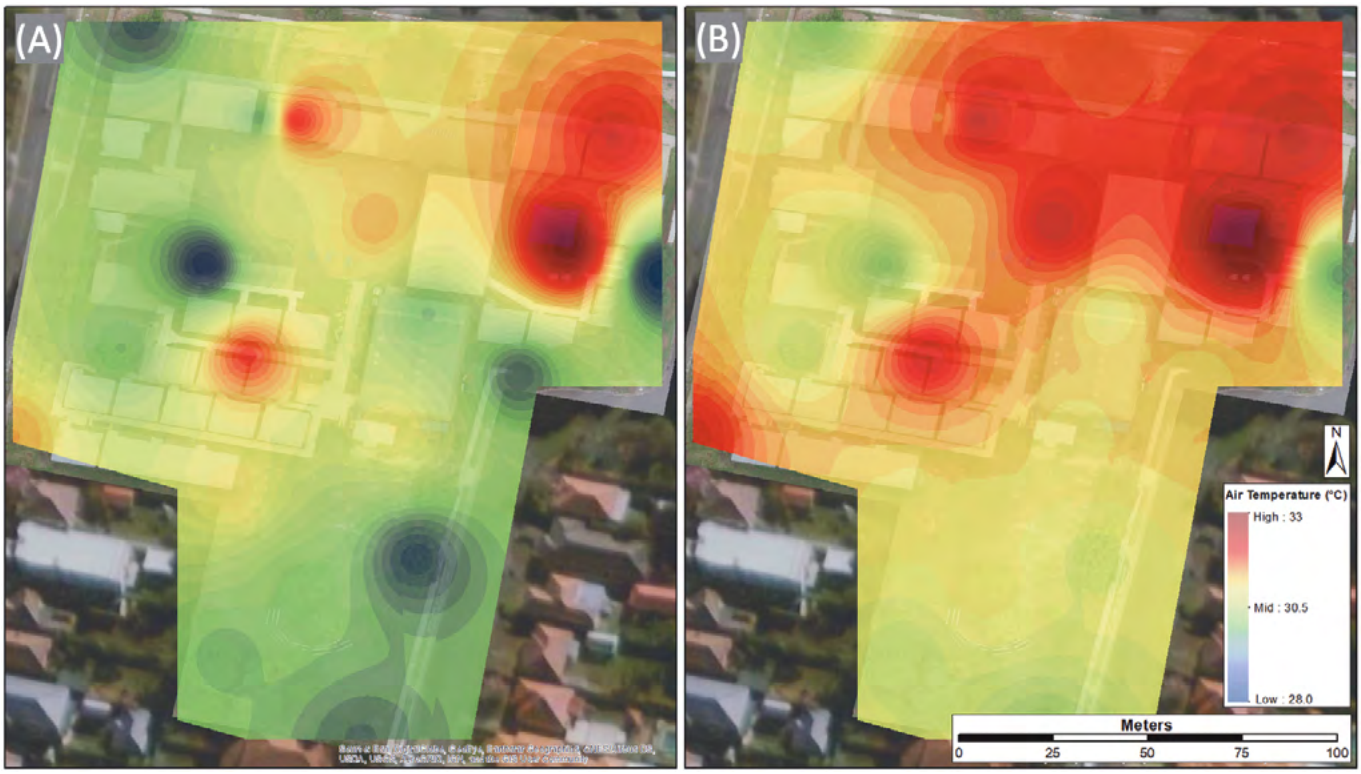

FIGURE 20: Interpolated temperature maps showing mean air temperatures across the school during (A) morning recess (11:10-11:40) and (B) the lunch and play time (13:20-14:10). For both time intervals, data spanning from 17 December 2019 to 26 January 2020 were averaged for 20 individual locations across the outdoor school environment.

Interpolated temperature maps of recess times show marked warming from late morning to lunch time (Fig. 20). With increasing absorption of solar radiation, all areas where corrugated iron sheets were used to provide shade became markedly warmer. Also, T_{air} across the central school yard rose and the overall temperature difference between the build environment and open, vegetated spaces the cool zone in the south and the hot zone in the north-east was diminished.

4.2.4 THERMAL COMFORT

Applying the NOAA Heat Index (HI) to the 20 continuous measurement locations resulted in an approximation of exposure to heat stress and, thus, thermal comfort. In keeping with previous information describing air temperature, the calculation of HI was based on data recorded during the operational hours (8:00-16:00) of the school.

The three locations that scored the highest number of hours where thermal comfort was low and associated heat risk was very high were, again, the playground, the small assembly area and the front of the library (Table 7). The total number of hours of extreme heat risk recorded at these three locations represented 34% of all hours recorded at the 20 locations across the school. This high proportion of time where children and adults could be exposed to extreme heat stress indicates that this section of the school is a hot spot and should be a focus area to implement strategies that can mitigate heat.

The area at the western side of the school near the driveway to the teacher's carpark had a large number of hours where the HI was high (45 hours) or moderate (77 hours), yet extreme HI scores were only recorded for 10 hours. This indicates that not only the hottest areas of the school should be thermally improved, but those that do not stand out during extreme conditions can have a severe impact on thermal comfort during school operating hours and should be considered for modification.

The two locations where the heat risk was at extreme levels for only a single hour during the entire project were under the pergola that was shaded by the large central tree (location H in Fig. 6) and at the front of the assembly hall (location I in Fig. 6).

TABLE 7: Number of hours (8:00 – 16:00) for a specific heat index level from 19 December 2019 to 26 January 2020. Please see temperature ranges for each risk level in Table 2.

LOCATION	SITE CHARACTERISTIC	HEAT RISK			
		EXTREME	HIGH	MODERATE	LOWER
G	Playground area	30	54	79	179
C	Assembly area	18	44	81	199
D	Pergola in front of library	18	39	79	206
L	Pergola between semi-permanent classrooms	16	41	69	216
N	Open space at toilet block	15	28	65	234
O	Open space at semi-permanent classroom	13	30	68	231
E	Central school yard (west)	12	30	63	237
T	Open space near driveway	10	45	77	210
F	Central school yard (east)	9	42	75	216
B	Passageway between buildings	7	31	55	249
K	*Lophostemon* tree	7	23	47	265
Q	*Lophostemon* tree	7	25	51	259
R	Grove of *Casuarina* trees	6	18	49	269
S	Grove of *Glochidion* trees	6	23	45	268
A	*Lagerstroemia* shrub	5	19	50	268
J	Grove of *Lophostemon* trees	5	19	41	277
M	Grove of *Lophostemon* trees	5	23	53	261
P	Row of *Ulmus* trees	5	20	48	269
H	Under pergola	1	15	48	278
I	Front area of Assembly Hall	1	19	57	265

4.2.5 IMPACT OF SHADE ON THERMAL COMFORT

Spot measurements of T_{air}, HI and T_{bg} were made to capture the effect of shade at five different locations around the school. The environmental conditions differed markedly during the three days. They were representative for a normal sunny summer day (14 January 2020), where mean T_{air} was below 29°C (Fig. 21). Measurements collected during the early afternoon of 30 December 2019 represented a very warm summer day, again with blue sky and mean air temperatures of close to 35°C. Measurements collected on 19 December 2019 were somewhat unusual. Although mean T_{air} was generally greater than 40°C (Fig. 21) making this a day of extreme heat, the sky across the Sydney Basin was covered by smoke from bushfires. Although some sunshine penetrated the smoke occasionally, the conditions were not representative for sunny conditions. However, overcast conditions are quite common during heatwave events in the Sydney Basin, making measurements collected on that day very valuable.

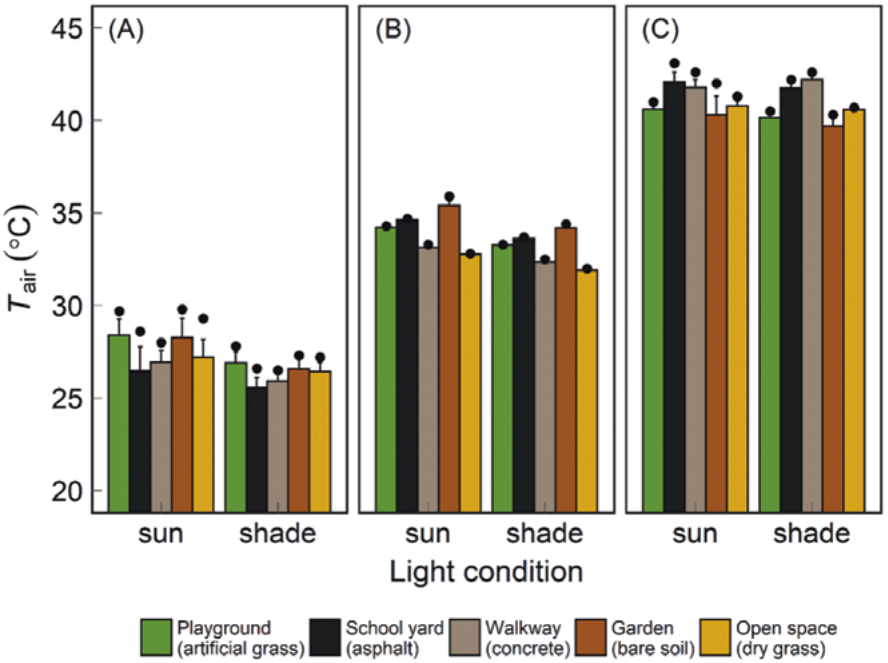

FIGURE 21: Mean air temperature (T_{air}) recorded in the sun and shade over five different surfaces during (A) a normal summer day (14 January 2020), (B) a hot summer day (30 December 2019) and (C) a day of extreme heat (19 December 2019). Locations and their respective surface materials are colour-coded as shown in the legend. Points represent maximum air temperature recorded for each surface and light condition. Values represent means (n = 10), error bars show 1 standard deviation from the mean, absolute maximum temperatures are shown as dots.

The effect of the overcast sky and resulting lower solar radiation can be seen in the reduced difference in T_{air} between sunlit and shaded positions on the day of extreme heat (panel C in Fig. 21). However, local mixing of air and the relative proximity of the sunlit and shaded position at each of the five measurement locations meant that shade did not generally reduce mean $T_{air.}$ Reductions were between 0.8 and 1.7°C on the normal and warm summer days. Although small in total difference, mean T_{air} was lower in shaded positions compared to the equivalent sunlit position at the same location and surface type during all three days.

During the normal summer day, the warmest mean T_{air} was measured in the playground where artificial grass was the dominant surface (28.4 ± 0.9°C) and in the front garden of the school where bare soil dominated (28.3 ± 1.1°C). Shading helped cool air temperatures at these locations by around 1.6°C. During the day of extreme heat, the highest mean T_{air} was 42.1°C (± 0.5), recorded in the central school yard over black asphalt. Here, shading only reduced mean T_{air} by 0.3°C. Reduction of mean T_{air} by shade was also low at all other locations that day, demonstrating the effect of bushfire smoke on blocking solar radiation.

While measurements of T_{air} did show some effect of shade on air temperature, this positive effect became clearer when analysing the effect on HI and T_{bg}. During the normal summer day, shading reduced the HI by up to 2.1°C and when averaged for all five locations, by 1.8°C. Slightly lower differences were measured for HI during the warm summer day where shade reduced HI by an average of 1.6°C. Lack of sunshine and very low relative humidity during the day of extreme heat resulted in reduction of HI across the five locations by 0.7°C. For the three days of measurements, the largest reduction in HI by shading was measured for the bare soil in the front garden of the school, while the smallest reduction of HI was calculated for the central school yard.

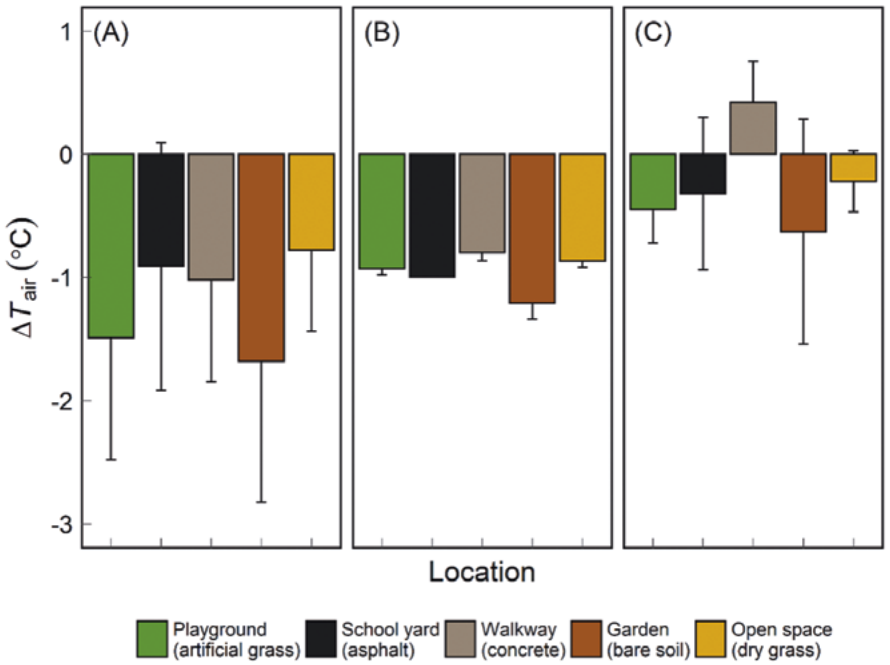

FIGURE 22: Difference in mean air temperature (ΔT_{air}) recorded in the sun and shade over five different surfaces during (A) a normal summer day (14 January 2020), (B) a hot summer day (30 December 2019) and (C) a day of extreme heat (19 December 2019). Locations and their respective surface materials are colour-coded as shown in the legend. Values represent means (n = 10), error bars show 1 standard deviation from the mean.

Temperature differences measured with the black globe thermometer were far greater. This was not surprising as this approximation of thermal comfort includes the impact of direct solar radiation and that of heat radiated from surfaces. The absolute highest 'feels like' temperature was 55.2°C measured on 19 December over the unshaded asphalt surface of the central school yard. During this day of extreme heat, the average effect of shading on mean T_{bg} was 6.7°C. Shading had the greatest effect on mean T_{bg} (11.5°C) over the concrete pathway between the semi-permanent classrooms measured on 30 December 2019 (the hot summer day).

Estimated across the normal, hot and extreme days, shading generated the largest reduction of mean T_{bg} for the school yard. This may seem contrary to the result reported above for HI as it had the smallest reduction at this location. However, it is important to note that HI is based on measurements of T_{air} and relative humidity, whereas T_{bg} takes radiation loads into account. Large thermal benefits and significant improvements of thermal comfort can therefore be achieved by shading black asphalt in the central school yard.

Only small improvements in lower T_{bg} would be achieved by further increasing shade in the open space at the southern end of the school. Here, reductions of mean T_{bg} were least when estimated across all three measurement days. This seems logical as the area already has the largest proportion of tree canopy area of the school, providing local shade and evaporative cooling.

It is highly informative to assess differences between measurements collected in the sun and shade in greater detail, as some observation are counter-intuitive, yet can markedly help planning for positive impacts on school thermal environments. In the following, information about the differential temperatures between measurements collected in the sun and shade (marked by a capital Greek letter delta, Δ) are provided. **Mean ΔTair is expressed as negative number to reflect the cooling effect of shade. More negative numbers indicate greater cooling as the difference between measurements recorded in sunlit positions and shaded positions increased.**

A general trend of decreasing mean ΔT_{air} with increasing heat was found (Fig. 22). While mean ΔT_{air} was -1.5°C and less around the playground and school garden on the normal summer day (14 January 2020), it was only about -1°C during the hot day (30 December 2019) and was even less reduced during the day of extreme heat (19 December 2019). The greatest effect of mean ΔT_{air} was on concrete, where all measurements during the extremely hot day resulted in positive values of mean ΔT_{air}. Positive values for Δ indicated that air temperatures over this surface material were warmer in the shade compared to those in the sun.

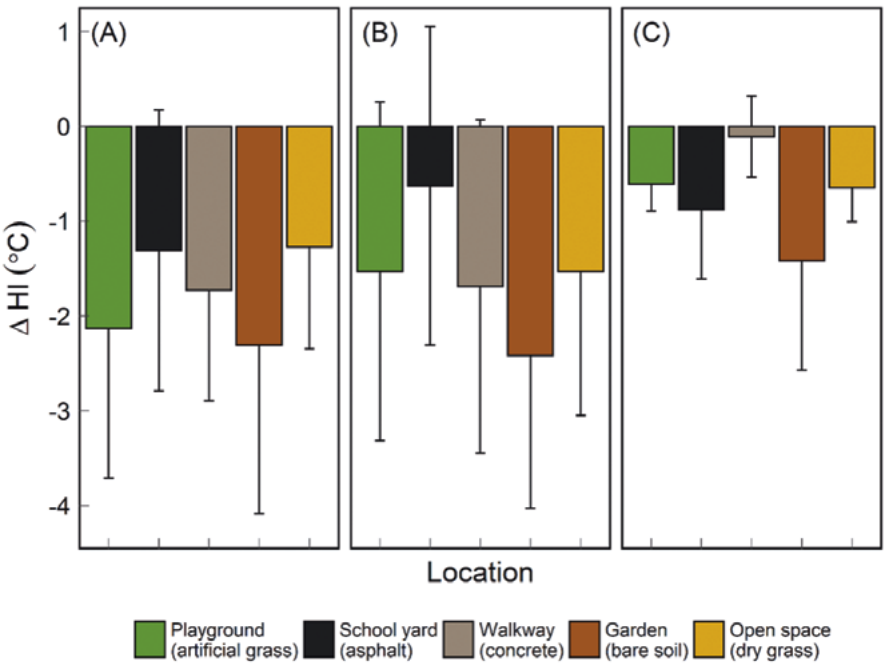

FIGURE 23: Difference in mean Heat Index (ΔHI) recorded in the sun and shade over five different surfaces during (A) a normal summer day (14 January 2020), (B) a hot summer day (30 December 2019) and (C) a day of extreme heat (19 December 2019). Locations and their respective surface materials are colour-coded as shown in the legend. Values represent means (n = 10), error bars show 1 standard deviation from the mean.

Differentials in the HI were also less negative during the day of extreme heat (Fig. 23). During the normal summer day, mean ΔHI on bare soil of the front garden was -2.3°C, but only -1.4 during the extreme heat day. Even more pronounced was the loss of cooling over concrete, where mean ΔHI increased from -1.7 to -0.1°C.

The most informative pattern of temperature reductions through shading were observed with the 'feels like' temperature of the black globe thermometer (Fig. 24). First, irrespective of changes in mean air temperatures over the three measurement days, shading of black asphalt always resulted in more than -10°C cooling of mean ΔT_{bg} (14 January 2020: -10.5°C; 30 December 2019: -10.1°C; 19 December 2019: -11.3°C).

A reduction in the effectiveness of shade to reduce mean ΔT_{bg} was found for measurements collected over the concrete surface (normal summer day: -11.5°C; hot summer day: -9.7°C; extreme summer day: -7.0°C) (Fig. 24). The opposite pattern, an increase in the cooling capacity of shade with increasing air temperature was measured for the garden in the front of the school where mean ΔT_{bg} was -4.6°C on the normal summer day compared to a bigger decrease of -9.3°C during the extremely hot day (Fig. 24).

Non-linear trends in mean ΔT_{bg} were found for both the playground area and the open space at the southern end of the school where cooling was most pronounced during the warm summer day (playground: -10.6°C; open space: -10.9°C), and less pronounced during the other two days (Fig. 24). Hence, it is likely that shading of artificial and dry grass can improve thermal comfort, particularly under sunny conditions. Once cloud cover (or, in the case of this study, smoke on the extreme heat day) prevents direct heating of these surface materials, their thermal benefits when shaded decline drastically.

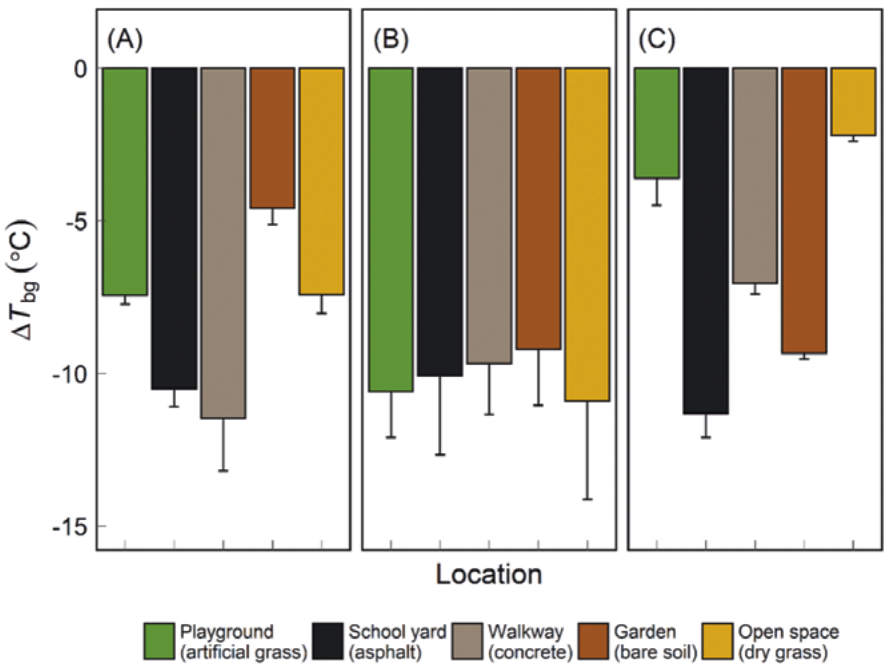

FIGURE 24: Difference in mean black globe temperature (ΔT_{bg}) recorded in the sun and shade over five different surfaces during (A) a normal summer day (14 January 2020), (B) a hot summer day (30 December 2019) and (C) a day of extreme heat (19 December 2019). Locations and their respective surface materials are colour-coded as shown in the legend. Values represent means (n = 10), error bars show 1 standard deviation from the mean.

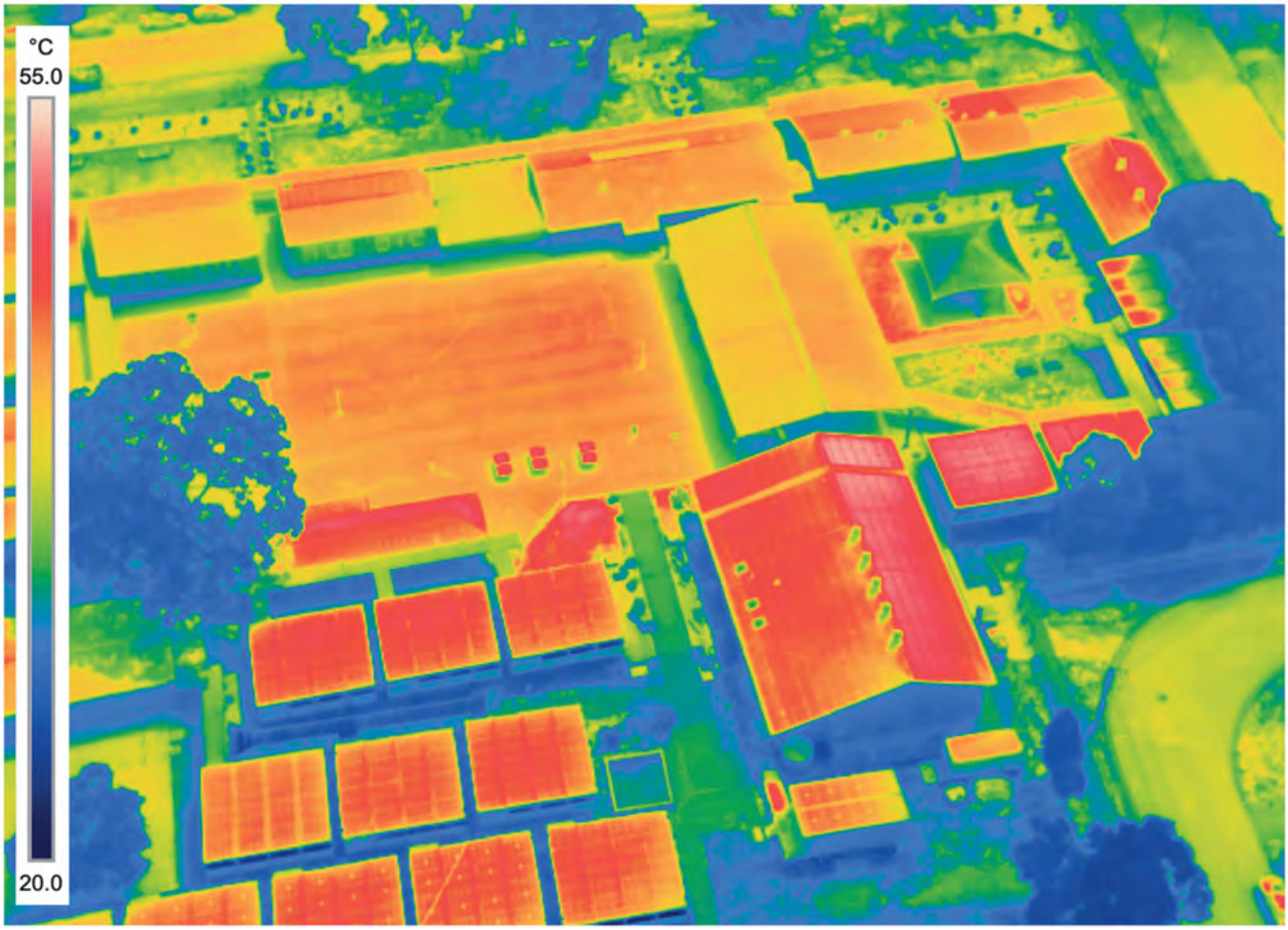

4.3 SURFACE TEMPERATURES

An aerial view of the school built environment revealed large differences among surface temperatures (Fig. 25). Generally, horizontal and angled roof areas, especially those of the semi-permanent classroom were hotter than most flat ground surfaces when in full sun. Also, hard surfaces of buildings and the central school yard were always warmer compared to vegetated surfaces and tree canopies. The hottest ground surfaces included the sunlit asphalt of the central school yard, sunlit artificial grass around the playground and sunlit bare soil in garden beds near the playground. The concrete surface of the central walkway connecting the school yard with the semi-permanent classrooms (area to the left of the assembly hall with blue-green colour in Fig. 25) was clearly cooler compared to asphalt of the yard.

FIGURE 25: Aerial infrared image of the northern section of the school. This section contains all administrative buildings, classrooms and the main school yard, playground and assembly hall. The image was taken at 11:00 on 27 January 2020. Image © S. Pfautsch

Assessment of surface temperature of different materials in full sunshine revealed that artificial grass and bare soil were the hottest surfaces, regardless of ambient temperatures (Table 8). Sunlit artificial grass reached a mean temperature of 52°C during the normal summer day despite the air temperature being below 30°C. The surface temperature of artificial grass increased when ambient air temperatures rose and a maximum value of close to 70°C was measured for this material (Table 8, Fig. 26). It should be noted that this material was used around the playground and two other areas near the semi-permanent classrooms. Bare soil showed similar dynamics when ambient T_{air} increased. A maximum surface temperature of 73°C was recorded on bare soil during the day of extreme heat.

While the sunlit asphalt surface of the school yard remained generally cooler than artificial grass or bare soil, this surface material showed the greatest difference in surface temperature (+9°C) for the normal summer day compared to the extremely hot summer day. In comparison, the difference in surface temperature of artificial grass and bare soil was 7.5 and 7.4°C, respectively (Table 8). Of all surface materials tested, sunlit concrete had the lowest surface temperatures on any day. During the day of extreme heat, the mean surface temperature of concrete was more than 15°C cooler compared to artificial grass (Table 6).

TABLE 8: Mean surface temperature of common surface materials measured in full sunshine around midday. Data were extracted from infrared images. Images were taken during midday of a normal (14 January 2020), hot (30 December 2019) and extremely hot summer day (19 December 2019). Values in parentheses indicate 1 standard deviation from the mean (n = 5). Maximum surface temperatures are single measurements.

GROUND SURFACE MATERIAL	NORMAL DAY (14 JANUARY 2020)	HOT DAY (30 DECEMBER 2019)	EXTREME DAY (19 DECEMBER 2019)	$T_{SURFACE\_MAX}$ (°C)
	$T_{surface}$ (°C)			
Artificial grass	51.7 (± 1.8)	56.1 (± 4.8)	59.2 (± 3.4)	67.5
Bare soil	49.5 (± 4.0)	55.7 (± 3.8)	57.1 (± 5.8)	73.4
Dry grass	49.4 (± 2.8)	46.8 (± 1.7)	51.4 (± 5.3)	60.0
Asphalt	44.8 (± 4.5)	51.1 (± 1.4)	54.4 (± 5.0)	61.6
Concrete	42.0 (± 5.3)	43.8 (± 9.3)	43.1 (± 4.3)	57.1

The lowest temperature measured for a ground material was the irrigated green lawn in the front garden of the school. During the day of extreme heat, this surface type reached a mean temperature of 38°C, being 20°C cooler than artificial grass or bare soil. Additional shading of green grass lowered the surface temperature of this material by another 4-5°C.

Green foliage of trees and shrubs displayed markedly cooler surface temperatures compared to hard ground surface materials. When air temperature was 43°C on the day of extreme heat (19 December 2019), leaves of trees displayed a mean surface temperature of 40°C. Lower leaf temperatures are the result of evaporative cooling and demonstrates the cooling potential of vegetation such that areas under or around tree canopy always had the lowest air temperatures (see Fig. 19).

Surface temperatures of vertical walls were lower compared to hard horizontal surfaces. Sunlit brick walls reached, on average, 34, 40 and 41°C during normal, hot and extreme summer days. Similar surface temperatures were measured for walls of the semi-permanent classrooms and the sheet metal walls of the buildings at the north-western section of the school. It is worth noting that the walls of the semi-permanent classrooms had the highest mean surface temperature (39°C) on the normal summer day for both sunny and shaded conditions.

Airborne imagery supported the thermal analyses of roof surfaces. Although these analyses were based on one sunny, warm summer day only (27 January 2020), clear differences in surface temperatures were found. These differences clearly related to material and colour of roofs. The green corrugated iron roof of the assembly hall and one administrative building showed the highest mean surface temperatures of 50°C with hotspots of 52°C. In comparison, mean surface temperature of beige coloured metal roofs of the COLA and one old, permanent classroom were 7°C lower, demonstrating the effect of colour and related absorbance and reflectance of solar radiation. The cement shingles of the roof of the main administrative building were cooler (45°C) than those measured for green (50°C) or corrugated iron roofs.

HOT AND COOL ZONES

On the following pages, a number of examples for *Hot Zones* and *Cool Zones*, as well as selected examples of surface temperatures of individual materials are provided. The term 'zone' is used here to clearly delineate selected areas across the school outdoor environment that are likely to represent higher or lower surface temperatures, and through radiation of heat also influence T_{air} and importantly also HI and T_{bg}. Therefore, the likelihood of children to experience heat stress is higher in a Hot Zone than in a Cool Zone.

The pairwise representation of a location as seen by the human eye and depicted as seen using an infrared filter and post-capture colouring. Colour-representation of surface temperatures was calibrated to the same temperature range in all infrared images.

Hot Zones (Fig. 26)

- Play areas covered by artificial grass (panels A and B): Sunlit artificial grass had a mean surface temperature of 61°C. When shaded, surface temperature of this material was 35°C and the adjacent shaded concrete path had a surface temperature of 29°C.
- Black asphalt (panels C and D): The large unshaded school yard made from black asphalt represented a local heat island. The image was taken during the late morning of a sunny day (23 January 2020) where air temperature was 34°C. Mean surface temperature of the entire area was 57°C and was 40°C when shaded (in the foreground).
- Non-vegetated ground (panels E and F): Between September and December 2019, Greater Sydney experienced an extended period of very low rainfall and high summer temperatures. The existing lawns of the open space at the southern end of the school died as result of drought and play activities. This left large patches of dry bare soil exposed to sunshine, reaching mean surface temperatures of 56°C during a day of extreme heat. Spot measurements showed surface temperatures of up to 64°C. In comparison, dry soil and grass that was shaded by a group of trees had a mean surface temperature of 39°C.

FIGURE 26: Hot zones around the school. On the left, images are shown as normal view. On the right the same location is depicted as seen through an infrared filter, visualising surface temperatures. Panels A/B: sunlit play area between semi-permanent classrooms covered with artificial grass. Panels C/D: sunlit central school yard made from black asphalt. Panels E/F: sunlit bare soil in the open area to the south. Images were taken on the extreme summer days where ambient air temperatures were well above 40°C (19 December 2019, panels A, B, E, F and 23 January 2020, panels C, D). Image© S. Pfautsch.

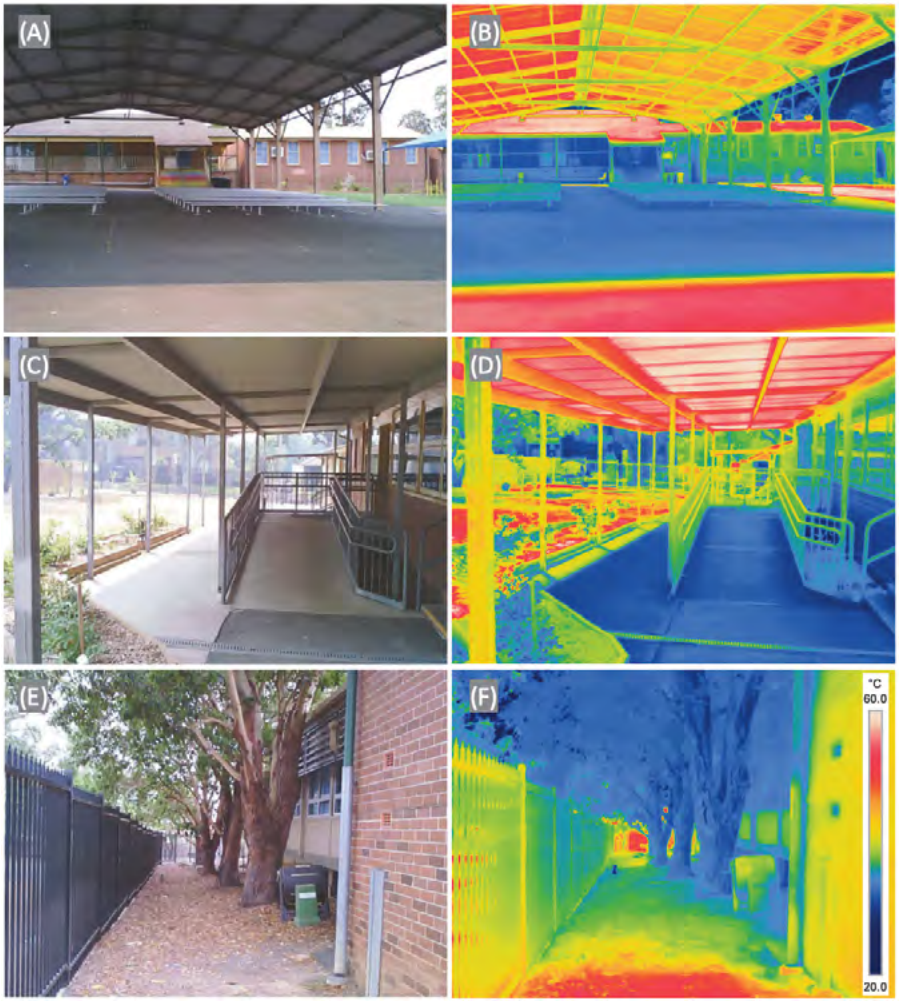

FIGURE 27: Cool zones around the school. On the left, images are shown as RGB. On the right the same location is depicted as seen through an infrared filter, visualising surface temperatures. Panels A/B: sunlit play area between semi-permanent classrooms covered with artificial grass. Panels C/D: sunlit central school yard made from black asphalt. Panels E/F: sunlit bare soil in the open area to the south. Images were taken on the extreme summer days where ambient air temperatures were well above 40°C (19 December 2019, panels A, B, E, F and 23 January 2020, panels C, D). Image© S. Pfautsch.

Cool Zones (Fig. 27)

- The large COLA (panels A and B): Shaded asphalt remained relatively cool during the day of extreme heat, reaching a surface temperature of 35°C. The metal roof above the sitting area was, on average, 49°C, however no signs of radiated heat from the roof towards the seating area were detected.
- Shaded walkways (panels C and D): Surface temperature of the shaded concrete walkways were relatively low (35°C) during a warm summer day, however, signs of radiated heat from the hot, uninsulated tin roof (surface temperature was 57°C) are visible on the handrails.
- Tree grove (panels E and F): Shaded surface, stems, canopy and classrooms were cooler at the eastern side of the school. Mean surface temperature of the ground was 28.7°C on the extremely hot day of 19 December 2019.

One example for a particularly hot surface material was the access ramp to the toilet blocks (panels A and B in Fig. 28). This metal ramp was coated with a dark anti-slip material for safety reasons. The material absorbs high quantities of solar radiation which the metal underneath absorbs and reradiates. Even on the extremely hot day (19 December 2019) when thick smoke was obstructing the sun during some parts of the day, the surface temperature of the ramp reached 67°C. It can be expected that the ramp will reach even higher surface temperatures during clear, hot summer days.

Well-watered plants usually transpire water during the day, which helps them to reduce leaf temperatures. As an example of this, the mean surface temperature of sunlit leaves of a perennial plant in the front garden of the school was 29°C (panels C and D in Fig. 28). In comparison, the dark bark mulch around the plant had a mean surface temperature of 49°C, with a maximum temperature of 56°C. Similarly, tomato vines in the school vegetable patch, which were in full sun, had a mean leaf

temperature of 29°C. These plants shaded the wall of the semi-permanent classroom, yet, their contribution to reducing T_{air} may have been limited due to the large patch of artificial grass with very high surface temperatures. This area in front of the planting containers reached maximum surface temperatures of 64°C, more than twice that of the plant foliage (panels E and F in Fig. 28).

Shading of horizontal ground surface materials had the greatest effect in reducing their temperature. Shade cooled down black asphalt by nearly 25°C (Fig. 29). This surface material displayed increasing temperature reductions under increasing ambient heat, indicating that shading becomes increasingly important during hot and extremely hot summer days. The same pattern was evident when artificial grass was shaded. During a normal summer day (14 January 2020), shade reduced the surface temperature of this material, on average, by 15°C, while during the extremely hot day, mean temperature reductions reached 18°C (Fig. 29).

Shading of bare soil also increased the effect of cooling under rising T_{air}, yet shading concrete did little to reduce the surface temperature of this material (Fig. 29). Concrete had the lowest mean surface temperature in the sun (Table 7), which helps explain the smaller reduction in surface temperatures when this material is shaded. Shading concrete during a normal and extremely hot day resulted in a reduction of 8°C, reducing the mean surface temperature from 42-43°C to 34-35°C.

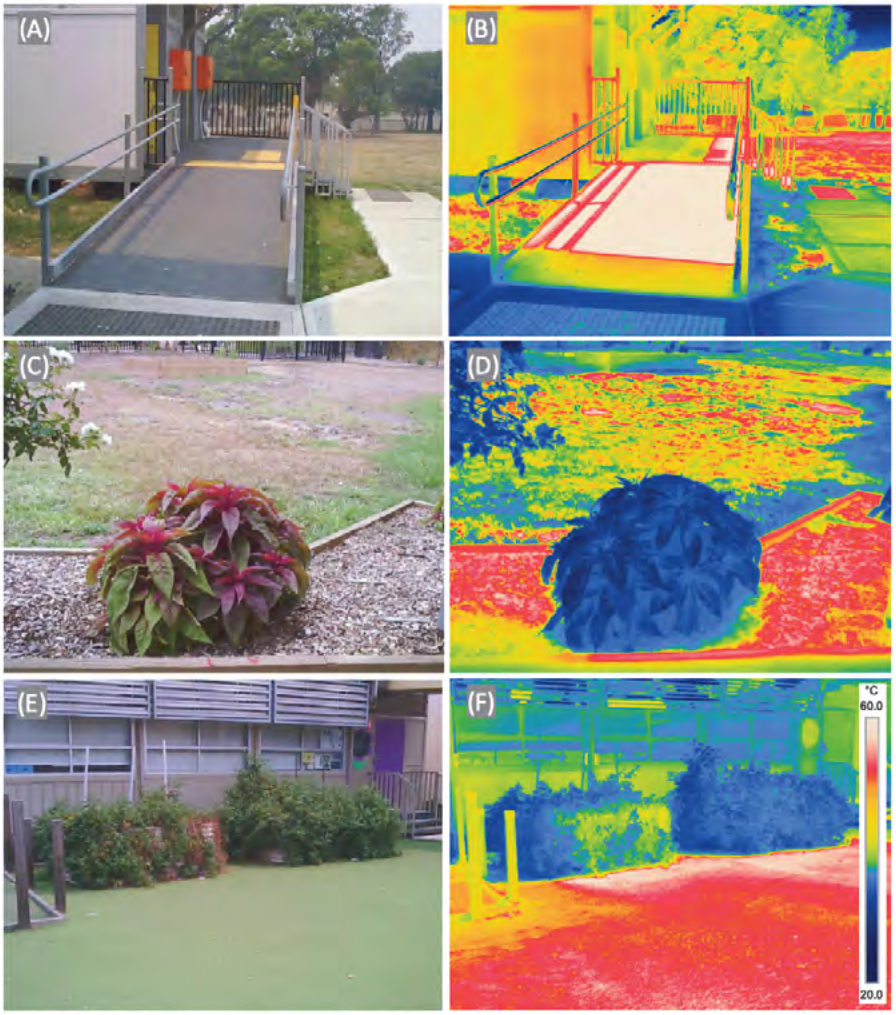

FIGURE 28: Examples of hot and cool objects across the school. On the left, images are shown as RGB. On the right the same location is depicted as seen through an infrared filter, visualising surface temperatures. Panels A/B: sunlit access ramp to toilet block. Panels C/D: sunlit, yet well-watered perennial plant in the front garden of the school. Panels E/F: sunlit tomato vines and artificial grass in front of a semi-permanent classroom. Images were taken on the extreme summer days where ambient air temperatures were well above 40°C (19 December 2019, panels A, B, E, F and 23 January 2020, panels C, D). Image© S. Pfautsch.

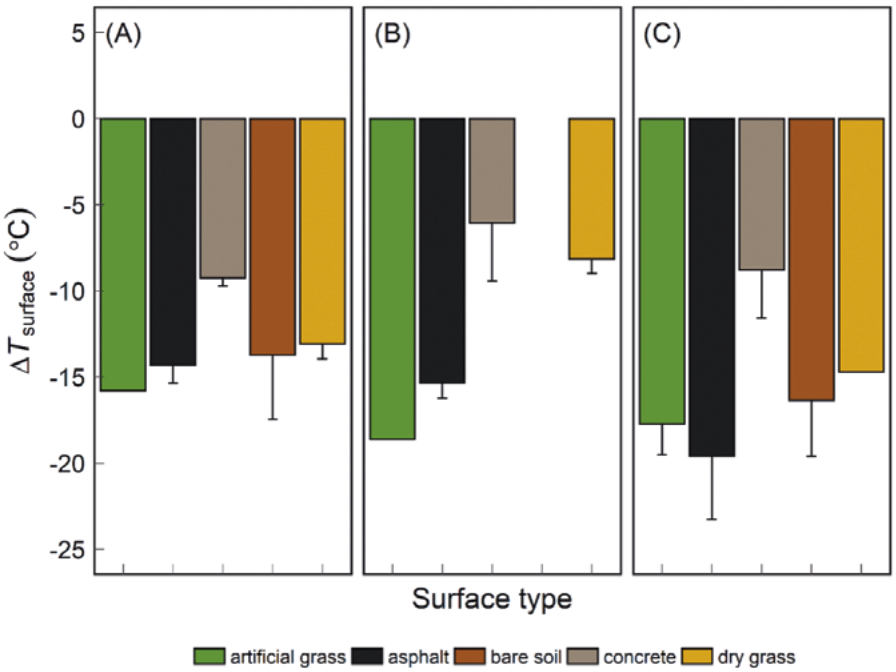

FIGURE 29: Difference in surface temperatures ($\Delta T_{surface}$) recorded in the sun and shade over five different surfaces during (A) a normal summer day (14 January 2020), (B) a hot summer day (30 December 2019) and (C) a day of extreme heat (19 December 2019). Locations and their respective surface materials are colour-coded as shown in the legend. Values represent means (n = 10), error bars show 1 standard deviation from the mean.

4.4 WATER REQUIREMENTS BY TREES

Despite the low rainfall in the months leading up to December, trees on the school grounds transpired substantial volumes of water. Mean daily water use was 54 L among the 10 trees investigated but varied largely depending on species and size. The largest tree included in these measurements was a mature Queensland Brush Box (*Lophostemon confertus*) located in the centre of the open space (tree 5 in Fig. 6 and Table 3 and 9). This large tree transpired an average of 156 L of water per day. Peak daily water use for this tree was 234 L measured on 21 January 2020. The Coast Banksia (*Banksia integrifolia*; tree 7 in Fig. 6 and Table 3 and 9) only used 9 L per day, which was the lowest volume for all trees measured.

TABLE 9: Water use of trees, recorded between 21 December 2019 and 12 January 2020 (measurement period 1) and 14 January 2020 and 26 January 2020 (measurement period 2). Tree IDs correspond with those listed in Table 3. Data in parenthesis show ± 1 standard deviation of the mean.

ID	SPECIES	COMMON NAME	MEASUREMENT PERIOD	MEAN DAILY WATER USE (L)	MAXIMUM DAILY WATER USE (L)
0	*Ulmus parvifolia*	Chinese Elm	1	34 (± 8)	56
1	*Lophostemon confertus*	Queensland Brush Box	1	20 (± 5)	28
2	*Ulmus parvifolia*	Chinese Elm	2	85 (± 35)	132
3	*Corymbia maculata*	Spotted Gum	2	83 (± 48)	161
4	*Ulmus parvifolia*	Chinese Elm	2	52 (± 16)	79
5	*Lophostemon confertus*	Queensland Brush Box	2	156 (± 55)	234
6	*Eucalyptus* sp.	Gum tree	1	94 (± 23)	134
7	*Banksia integrifolia*	Coast Banksia	1	9 (± 2)	16
8	*Allocasuarina* sp.	Sheoak	2	38 (± 20)	74
9	*Glochidion ferdinandi*	Cheese Tree	1	32 (± 14)	65

Responses to environmental conditions differed among the species, especially on days with extremely high air temperatures combined with very low relative humidity (e.g. 31 December 2019 and 4 January 2020, where air temperatures rose above 40°C). During these two days, driven by very low relative humidity, VPD rose above 8 kPa, presenting atmospheric conditions commonly found in deserts (Fig. 30A). Transpiration of the Cheese Tree (*Glochidion ferdinandi*) followed VPD well and more than doubled during days of high VPD and air temperature (Fig. 30B). However, water use of a nearby eucalypt was unaffected and remained high before, during and after days of extreme heat (Fig. 30C). A cool change following the extreme heat of 4 January 2020 reduced water use among all trees as VPD was very low the following day (5 January 2020).

Mean daily water use of the remaining eight trees was 54 L per tree. If multiplied across the entire tree population of the school (n = 69), the daily water use of all trees would be around 3,700 L on a warm, sunny summer day. This is a very crude estimate of daily water use of trees across the school grounds. However, it is a useful indicator to gauge the magnitude of soil water taken up by trees and transpired into the atmosphere. Trees around school buildings and open spaces certainly contributed to lowering ambient air temperatures through shading and transpiration of a noticeable amount of water drawn from the soil.

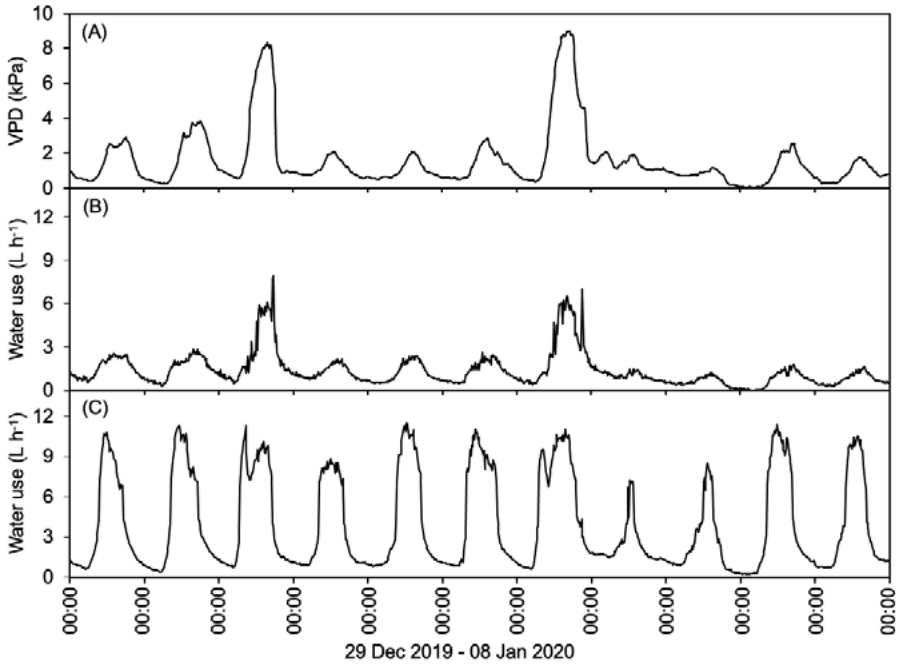

FIGURE 30: Extreme environmental conditions and the response of tree water use. (A) Vapor pressure deficit (VPD) of the atmosphere. (B) 24-hour cycles of tree water use of Cheese Tree (*Glochidion ferdinandi*; tree 9 in Table 3) and (C) *Eucalyptus* sp. (tree 6 in Table 3).

4.5 **TREE SPECIES ENDORSEMENT**

For each of the scenarios tested, safety, limb drop and an allrounder tree, Jacaranda was ranked as the most suitable (Table 10). When prevention of limb-drop was given a high preference, both Weeping Lilly Pilly (*Syzygium floribundum*) and Weeping Bottlebrush (*Callistemon viminalis*) scored highly. When selecting for an 'allrounder', a species that met many criteria to be a safe, shady species with a low risk of being poisonous or produce allergens, all species were medium sized trees that could grow up to 15 m in height and provide good quality shade. Given the right management, Jacaranda and other non-native, deciduous species like *Plantanus* (London Planetree), Acer (Maple) or *Liriodendron tulipifera* (Tulip Tree) would be suitable as feature trees that can provide cooling and other benefits in school yards.

TABLE 10: Outcome of the three scenarios to select the ten most recommendable tree species for planting in schools across Western Sydney. Species were selected from the 30 most abundant street tree species identified in the area. The weighing of each of seven factors to assess the suitability of each species is shown in Table 5.

SCENARIO 1: MULTIPLE SAFETY ASPECTS	SCENARIO 2: WITHOUT LIMB DROP	SCENARIO 3: 'ALLROUNDER'
Jacaranda mimosifolia	*Jacaranda mimosifolia*	*Jacaranda mimosifolia*
Syzygium floribundum	*Syzygium floribundum*	*Callistemon viminalis*
Callistemon viminalis	*Callistemon viminalis*	*Lophostemon confertus*
Lophostemon confertus	*Lophostemon confertus*	*Tristaniopsis laurina*
Tristaniopsis laurina	*Tristaniopsis laurina*	*Callistemon citrinus*
Lagerstroemia indica	*Lagerstroemia indica*	*Melaleuca quinquenervia*
Elaeocarpus reticulatus	*Elaeocarpus reticulatus*	*Syzygium floribundum*
Prunus cerasifera	*Callistemon citrinus*	*Prunus cerasifera*
Syzygium smithii	*Melaleuca quinquenervia*	*Syzygium smithii*
Melaleuca bracteata	*Prunus cerasifera*	*Lagerstroemia indica*

5. CONCLUSIONS & RECOMMENDATIONS

This project documented summer heat at a public school in Western Sydney at a level of detail that is novel for any school in Australia. The intention of this project was to not only identify hot and cool zones around this particular school, but to showcase how microclimate assessments can help to identify thermal performance of new and existing outdoor school environments. It is acknowledged that measurements reported here were collected during the summer holidays. Yet, according to climate change predictions, the recorded conditions will be come more frequent and likely to occur more during times when schools are operational. Hence, results of this study also provide a valuable 'outlook' to microclimatic conditions schools will have to deal with in the near future.

The following recommendations are intended to assist architects, planners and landscape designers to create heat-smart school yards. The recommendations are also useful for principals, school managers and ground staff to identify areas and structures that can be modified to mitigate summer heat and eliminate potential hazards for burn injuries and heat stress of students (and teachers) during increasingly hot summer conditions. Finally, our innovative heat maps can be used to develop evidence-based strategies how to plan and regulate outdoor play during recess times on hot summer days.

As a result of the dependency of near-surface air temperature and human thermal comfort on a range of factors that originate from characteristics of the natural and built environment, it is important to assess school microclimates holistically. The combined assessment of material characteristics and shade or sun exposure reveal not only why a particular space is hotter than another, it also indicates how to improve the thermal environment around a specific location.

5.1 REDUCING RADIANT HEAT

Shade, either natural or artificial, reduces surface temperatures. Lower surface temperatures result in reduced emission of stored energy that in turn will improve thermal comfort and lower the risk of heat-related incidents. We provide examples how heat can be reduced through insulation, shading, improved ventilation and replacement of surface materials.

High air temperatures for the entire measurement period were recorded under the walkway in front of the library. Orientation of this location was towards north, with full exposure to midday and afternoon sunshine. Shade at the location was provided by a pergola, which should have reduced the impact of direct solar radiation. Detailed assessments using infrared thermography revealed that the pergola indeed resulted in cool surface temperatures of the concrete walkway underneath it, but high radiant heat from the metal roofing material caused additional heating of the air underneath the shade structure. Here, thermal comfort can be improved by insulating the underside of the metal roof, or by including a barrier that absorbs the radiated heat. This barrier could be made from light-coloured wooden slats, attached to the supporting structure of the pergola. Moreover, the upper, sun-exposed surface of the pergola could be coated with a highly reflective surface coating (i.e., cool roof paint) to reduce the amount of heat absorbed and emitted.

The cooling effect of shade on the pergola roof was demonstrated at measurement location H. This location was shaded by the large white mahogany tree in the south west of the central school yard where mean summer air temperature was 1°C lower compared to the location D in front of the library.

Equally simple, cost-effective solutions could be used to improve the thermal environment of the school playground. Paradoxically, this area where children are invited to spend prolonged time for outdoor play was the top hotspot of the entire school. The location of the playground, being surrounded by solid buildings on three sides and the large roof and supporting structure of the COLA on the fourth side reduced air flow in the playground. While this situation is difficult to change, alteration of surface and shade materials would help to mitigate heat in the playground. Unshaded artificial grass was one of the hottest surface materials across the school. Higher surface temperatures and greater rates of longwave radiation from this material, compared to asphalt, concrete and turf have been demonstrated in systematic studies (Yaghoobian et al., 2010). Shading or replacing this material with a heat-inert alternative would certainly help reducing its contribution to sensible heat.

Opening the canopy above the playground would deliver additional benefits. Currently the closed pitched-roof canopy covered by dark shade cloth traps hot air. The combined effect of preventing convection of this heated air, combined with continuous heating of air by radiation from artificial grass leads to the highest number of hours where the HI was at extreme or high levels of health risk. Alternative shade structures are commercially available that provide protection from UV radiation to keep surfaces cool while allowing hot air to escape (e.g., hypar shade sails).

The issue of trapped heat was also noticeable in the small assembly area at location C. Similar to the canopy over the playground, this pitched, grey corrugated metal roof did not permit sufficient ventilation of the upper airspace. Installation of two to three roof turbine vents or other products that allow trapped heat to escape will improve natural ventilation and thermal comfort in this location.

To reduce the additional warming from radiated and trapped heat we recommend:

- Materials used for shading should be of light colour
- Metal roofs should be coated (top side) and/or insulated (underside)
- Shade structures that cannot be light coloured, coated or insulated should be sufficiently high above the ground to prevent noticeable radiation of sensible heat
- Natural air flows should not be obstructed
- Use of artificial grass should be avoided or restricted to areas with zero exposure to direct sunshine
- Shade should cover the entire playground and assembly area
- Where possible, replace closed with open shade structures that allow hot air to dissipate through convection (e.g., Whirlybird, Creative Heat Vent, Solar Vent)
- In addition, playground equipment made from materials that do not absorb and conduct heat well (e.g., wood) could be provided

5.2 **FOCUS: ASPHALT**

Materials like asphalt and concrete are commonly used to cover surfaces around schools. These materials have a low albedo (i.e., low reflectivity) and a high volumetric heat capacity (i.e., capacity to absorb, store and emit heat). Surface temperatures of these materials easily exceed 60°C on hot summer days (Mohanjerani et al. 2017). Many school yards and other flat spaces in schools are made from black asphalt, including driveways, walkways, lanes and carparks. Compared to other surface materials, asphalt is a low-cost material that requires little maintenance, is durable, easy to clean and relatively cheap to repair and replace. Yet, as shown by our terrestrial and airborne measurements of surface temperatures, unshaded asphalt represents a noticeable source of radiant heat. Shading asphalt reduced black globe temperatures by more than 10°C and lowered the HI by 2°C. Surface temperature of asphalt even during the normal summer day was above 60°C. Such surface temperatures clearly represent a hazard risk for skin burns if contact time exceeds just 5 seconds (ISO 13732, 2010).

To reduce radiated heat and burn hazards from asphalt (and other hot surface materials like artificial grass and coated metal) we recommend:

- Shade surfaces with trees (e.g., Jacaranda Weeping Lilly Pilly, but also consider maples or tulip trees), fabric shade sails or hard roofs
- Where impact attenuation is necessary, use only light-coloured softfall rubber materials of highly reflective polymer products (products like **Polysoft**)
- Where possible, replace surface materials with light coloured alternatives (pavers, recycled concrete, sand), or engineered surface materials (products like **Flow Stone**)
- Coat sun exposed asphalt and metal surfaces with heat reflective surface sealants (products like **Cool Seal**, **Cool Pave** or **Street Bond**)

5.3 **INCREASING TREE CANOPY COVER**

The 69 trees around the school covered only 20% of the total area of the school. None of the buildings in the northern section of the school and none of the semi-permanent classrooms south of the central school yard received any shade from trees. Equally, the central school yard and large parts of the open space in the southern section of the school were unshaded. We showed that shading reduced surface temperatures in the central schoolyard by more than 20°C during summer. Shading other surface types reduced their temperature by 10-15°C.

When surfaces were shaded, their radiant heat loads were reduced and this contributed to an increase in thermal comfort, lower 'feels like' temperatures and reduced HI temperatures of more than 2°C. Clearly, shading more surface area and buildings will decrease the risk of heat-related illnesses at the school during increasingly hotter summers.

The cooling effect of trees on air and surface temperatures as well as human thermal comfort is well established (Sanusi et al., 2017). A positive effect is especially pronounced on hard surfaces, including asphalt, roofs and walls of buildings (Gillner et al., 2015). An ever-increasing number of studies show that air and surface temperatures in urban environments, like schools, can be reduced if tree canopy cover is expanded (Aram et al., 2019; Ziter et al., 2019). Hence, increasing tree canopy cover across the school, using trees that are safe (i.e., do not drop green limbs, non-allergenic and non-poisonous), tall and form a large, dense crown will provide additional shade and cooling. Our tree selection tool has identified that several tree species, particularly Jacaranda and Weeping Lilly Pilly meet these criteria. However, other trees such as bottlebrushes, Queensland Brush Box or paperbarks are well suited for planting in school yards too.

Generally, adding trees to an unshaded school environment provides the best cooling benefits (Antoniadis et al., 2016, 2018). However, we have shown that canopy area and transpiration vary according to species and size of trees. Differences also exist in the response of trees to extreme heat. Some species increase their water use to provide additional cooling of their leaves. Others maintain a generally high level of transpiration and continue to provide transpirative cooling benefits even during extreme summer heat (Drake et al., 2018). Such species differences should be considered when selecting tree species for planting around schools. Also, sufficient water must be supplied to all existing and especially any newly planted trees to maintain high rates of transpiration and support tree establishment. High rates of transpiration will provide the maximum thermal benefits through latent heat flux cooling. Fast growing trees will provide a larger canopy for shade in a shorter amount for time.

To increase the area of tree shade and transpirative cooling, we recommend:

- Planting of advanced trees for fast expansion of tree canopy
- Select suitable species – consider safety, allergens, crown shape and size at maturity, location and maintenance requirements
- Selection of resilient species - selection of tree species should take into account if species can cope with hotter, drier climates expected with climate change.
- Strategic tree planting to shade buildings in the north and reduce heat in hot zones
- Construct large tree planting pits at the outer perimeter of the central school yard to increase shade of the yard and adjacent buildings
- Use of collected rainwater to irrigate trees during dry and hot summers

It is acknowledged that additional tree canopy will take time to develop. An intermediate alternative is to provide shade in hot zones through green pergolas. These structures are relatively easy to erect and well-watered climbing plants will provide green, leafy cover quickly.

5.4 **GREENING-UP**

Similar to trees, ground vegetation can improve microclimatic conditions through evapotranspiration and transfer beneficial effects on human health and thermal comfort by decreasing near-surface air temperatures (Antoniadis et al., 2018). Additional greening around the school can also improve general well-being and encourage physical activity (Onori et al., 2018). Hence, healthy, green vegetation is one of the most effective methods to minimise heat stress and has additional benefits of increased student and teacher well-being. The dry and hot conditions during spring and early summer 2019/2020 left large tracts of open space either covered in dry grass or even bare soil. Our measurements documented that these areas were markedly hotter compared to those where green grass had prevailed. Bare soil reached maximum surface temperatures of more than 73°C. At the same day and time of measurement, surface temperatures of green grass in the school garden were 40°C cooler. Further, all green surfaces of plants (i.e., leaves, canopy) had lower surface temperatures than any hard surface of building material during all three measurement days.

Keeping lawns green and covering exposed soil in garden beds will help reduce thermal loads across the school. For this reason, we recommend:

- Installation of an irrigation system in the front garden and the open space in the south (e.g., subsurface turf wicking using products like **KISSS**)
- Use water from existing rainwater tanks to maintain green plant cover around the school, especially around the playground to reduce thermal loads in this hot zone where air flows are low
- Increase the amount of rainwater tanks to collect additional runoff from roofs to supplement plant irrigation of garden beds and vegetable planters
- Replace impervious surfaces with fast-growing C-4 grasses to generate reductions of surface heat immediately; this approach works best if irrigation is provided
- Use green trellises to minimise the impact of heat on building walls; this approach works best if irrigation is provided

Maintaining continuous lawn cover during summer can be challenging, especially for schools where enrollment numbers are high and the area of green outdoor space is small. Under these conditions, grassed areas are under high pressure and will require additional maintenance. In addition, water restrictions during hot, dry summers will further limit the capacity of schools to maintain continuous lawn cover. Increasing the capacity to collect rain water and recycle grey water would help improving this situation.

5.5 **REDUCING ANTHROPOGENIC HEAT**

Air conditioning units increase ambient temperatures by releasing waste heat (Salamanca et al., 2014). All semi-permanent classrooms in the south of the central school yard feature air conditioning units. The classrooms are arranged in tight rows and the air conditioning units are installed at the southern side of each classroom. While the location of the units means they remain shaded during school operating hours, their venting systems release heated air into the confined space between classrooms. The tight spacing of the classrooms minimise natural ventilation of the area and release of waste heat by the air conditioning units increases ambient air temperature around access paths and classroom doors and windows.

All semi-permanent classrooms have flat roofs that heated up quickly to high temperatures (>50°C). The walls of the classrooms regularly showed surface temperatures of >44°C. The combination of high ambient air temperature, hot roofs and walls and additional heat generated by air conditioning systems generates a perpetual warming cycle and increasing energy use for cooling (Salamanca et al., 2014). The configuration of infrastructure in the area, including pergolas (identical to the one at the library) that radiate additional heat increases the chance of heat stress during the hottest periods in summer and increases energy consumption.

Low-intensity green roofs can easily be retro-fitted to existing roofs (Downton, 2013) and help improve urban microclimates (Razzaghmanesh et al., 2016). These types of green roofs typically have shallow soil systems (<200 mm), adding little additional weight to the supporting structure. They also are not irrigated and for this reason support low maintenance, drought tolerant vegetation. Establishing low-intensity green roofs on semi-permanent classrooms is an option that will reduce ambient air temperatures through evaporation of stored water and insulate

the classrooms against transmitted heat. Transforming conventional flat roofs to green roofs also minimises surface temperature variability, reducing cooling requirements in summer and heating requirements in the winter (Bevilacqua et al., 2017).

To reduce anthropogenic heat in the area, we recommend:

- Retrofitting air conditioning vents to release heated air vertically, not horizontally
- Covering roofs of semi-permanent classrooms with high albedo material
- Consider transformation to low-intensity green roofs

5.6 HEAT MANAGEMENT

Measurements collected around the school indicate that hazardous microclimates do exist on some days. Hazards and risks related to extreme air temperatures during heatwaves will remain and increase in frequency, magnitude and duration (CSIRO and Bureau of Meteorology, 2015). While these hazards and risks can only be mitigated through global efforts to reduce the greenhouse effect, a large number of practical recommendations are provided to help improve microclimatic conditions around the school. These recommendations aim at reducing surface heat, expand shade and improve the thermal comfort of children (and adults).

During summer, regular, sufficient and potentially supervised consumption of water should be the very first and cheapest strategy to reduce alarmingly common dehydration of school children in warm and hot climates (see Bar-David et al., 2009 and references therein). A more refined tool to improve heat management strategies are the new microclimate maps.

The maps depicting near-surface air temperatures during morning recess and lunchtime identify areas where children are exposed to high heat loads. Knowing about these hot zones allows teachers and other school personnel to develop strategies for outdoor activities that reduce heat loads during hot and extremely hot days. Activities in hot zones can also be time-limited and activities can be shifted to take place in cool zones. Education about the existence of hot zones can result in improved self-management of children.

General heat management strategies and actions can be developed and implemented during days where extreme heat is forecasted. Such strategies can include (1) shifting of recess times to earlier parts of the day, (2) invest in equipment that can provide chilled drinking water and ice cubes to help lowering core temperature of children, (3) provide activities in cool zones, (4) close-off the open space to limit gross motor activities and (5) increase seating and perching facilities in cool zones and shaded areas.

5.7 DESIGNING NEW SCHOOL INFRASTRUCTURE

Adaptation and mitigation must be leading concepts when designing new school infrastructure that can cope with the effects of climate change, particularly increased summer heat. Similar to large infrastructure construction projects, newbuild school infrastructure should follow the principle of 'Do No Harm' (Alteshuler and Luberoff, 2003). Incorporating air conditioning for classrooms, offices and other indoor spaces of schools will be essential to provide adequate learning conditions. Equally essential will be strategies that help reduce energy consumption and release of anthropogenic heat, and improve school outdoor microclimates, create safe spaces for outdoor learning and play and prevent physical harm. From a socio-ecological viewpoint, it would be advisable to provide adequate cool 'in-between spaces', as these spaces are important for self-directed play and associated learning (Aminpour et al., 2020).

Factors such as tree canopy cover, building and landscape design, orientation of buildings and selection of make and colour of materials will greatly improve the thermal performance of new school infrastructure. Beyond the consideration of heat-smart schools, we also advocate that incorporating techniques to improve the resilience and sustainable operation of new school infrastructure should be carefully evaluated for each project. These include, but are not limited to:

1. Generation of renewable energy
2. Collection and reusing of rainwater
3. Recycling of grey water
4. Passive cooling strategies for buildings
5. Water-sensitive design of outdoor spaces
6. Potential for green façades, breathing walls and green roofs
7. Incorporation of existing green infrastructure, especially large canopy trees
8. Optimal protection against direct and reflected UV radiation.

5.8 COOL SCHOOL RESEARCH

This project is the first of its kind. To our knowledge, the outdoor microclimate of a public school has never been studied at the level of detail presented here. Summer heat is increasing in Australia, making it necessary to understand how increasingly harsh environmental conditions will impact the opportunities of children to achieve their full potential. Heat reduces learning outcomes (Goodman et al., 2018) and providing a suitable learning environment inside and outside classrooms will be essential to maintain a level of education that guarantees our future knowledge capital.

There is a clear need for more evidence-based research to better understand the impacts of heat in schools, including the exact mechanisms that result in lower cognitive capacity under thermal stress (Gaoua, 2010). Given the high sensitivity of children's health to heat, it is astonishing that no national or international standards for thermal comfort of children exist (Madden et al., 2018). Our lack of assessment of how ambient environmental conditions impacts well-being

and physiological and cognitive abilities of children prevents us from formulating practical adaptation policies and guidelines (Vanos, 2017).

Research is also necessary to help establish comprehensive and systematic guidelines for the construction of heat-smart school infrastructure. Design of school buildings, school yards, playgrounds, gardens and other open spaces should incorporate evidence-based cooling principles. While the positive cooling benefits of shade, tree canopy cover, reflective materials or irrigation have been described in the scientific literature, their application in school environments is yet to be quantified.

Unknowns include:

- What is the optimal area of shade for a given school?
- Do cooling benefits differ if shade is provided by trees or metal roof structures?
- How much water will be needed to maintain high transpiration rates of growing trees?
- If cooler school outdoor environments are provided, will both genders benefit equally? Research has shown that redesigning and retrofitting school yards may not stimulate physical activity equally (Andersen et al., 2019).

Well-designed quantitative and qualitative research can provide answers to these and many other questions around the impact of heat on children and school infrastructure. Understanding how global warming is impacting human capital, embodied in student's learning outcomes and achievements is improving (Roach and Whitney, 2019). In a warming world it is a fundamental requirement to counter the negative impacts of heat on learning by providing heat-smart outdoor learning environments where children thrive.

6. LITERATURE INDEX

Altshuler, A., Luberoff, D. 2003. *Mega-projects: the changing politics of urban public investment*. Brookings Institutions Press, Washington, DC, United States, 352 p.

Aminpour, F., Bishop, K., Corkery, L. 2020. The hidden value of in-between spaces for children's self-directed play within outdoor school environments. *Landscape and Urban Planning* 194: article 103683.

Andersen, H. B., Christiansen, L. B., Pawlowski, C. S., Schipperijin, J. 2019. What we build makes a difference – mapping activating schoolyards features after renewal using GIS, GPS and accelerometers. *Landscape and Urban Planning* 191: article 103617.

Antoniadis, D., Katsoulas, N., Papanastasiou, D., Christidou, V., Kittas, C. 2016. Evaluation of thermal perception in schoolyards under Mediterranean climate conditions. *International Journal of Biometeorology* 60: 319-334.

Antoniadis, D., Katsoulas, N., Kittas, C. 2018. Simulation of schoolyards' microclimate and human thermal comfort under Mediterranean climate conditions: effects of trees and green structures. *International Journal of Biometeorology* 62: 2025-2036.

Aram, F., Higueras Garcia, E., Solgi, E., Mansournia, S. 2019. Urban green space cooling effect in cities. *Heliyon* 5: e01339

Atha, W. F. 2013. Heat-Related Illness. *Emergency Medicine Clinics of North America* 31: 1097-1108.

Baker, J., Gladstone, N. 2018. *Where summer is stifling: the NSW schools with and without air-con*. Sydney Morning Herald, 12 July 2018. Accessed 25 May 2020 at: https://www.smh.com.au/politics/nsw/where-summer-is-stifling-the-nsw-schools-with-and-without-air-con-20180711-p4zqsx.html.

Bar-David, Y., Urkin, J., Landau, D., Bar-David, Z., Pilpel, D. 2009. Voluntary dehydration among elementary school children residing in a hot arid environment. *Journal of Human Nutrition and Dietetics* 22: 455-460.

Bevilacqua, P., Mazzeo, D., Bruno, R., Arcuri, N. 2017. Surface temperature analysis of an extensive green roof for the mitigation of urban heat island in southern Mediterranean climate. *Energy and Buildings* 150: 318-327.

Brockman, R., Jago, R., Fox, K. 2011. Children's active play: self-reported motivators, barriers and facilitator. *BMC Public Health* 11: 461-467.

Cedeño Laurent, J. G., Williams, A., Oulhote, Y., Zanobetti, A., Allen, J. G., Spengler, J. D. 2018. Reduced cognitive function during a heat wave among residents of non-air-conditioned buildings: an observational study of young adults in the summer of 2016. *PLoS Med* 15: e1002605.

Coates, L., Haynes, K., O'Brien, J., McAnneney, J., De Oliveira, F. 2014. Exploring 167 years of vulnerability: an examination of extreme heat events in Australia 1844-2010. *Environmental Science & Policy* 42: 33-44.

CSIRO and Bureau of Meteorology. 2015. *Climate change in Australia: information for Australia's natural resource management regions*. Technical Report, Commonwealth Scientific and Industrial Research Organisation and Bureau of Meteorology, Canberra, Australia, 222 p.

De Dear, R., Kim, J., Candido, C., Deuble, M. 2015. Adaptive thermal comfort in Australian school classrooms. *Building Research & Information* 43: 383-398.

Downton, P. .2013. Green roofs and walls. *Your home - Australia's guide to environmentally sustainable houses.* Australian Government. Accessed 07 February 2020 at: https://www.yourhome.gov.au/materials/green-roofs-and-walls.

Drake, J. E., Tjoelker, M. G., Varhammar, A., Medlyn, B., Reich, P.B., Leigh, A., Pfautsch, S., Blackman, C. J., Lopez, R., Aspinwall, M. J., Crous, K. Y., Duursma, R. A., Kumarathunge, D., de Kauwe, M. G., Jiang, M., Nicorta, A. B., Tissue, D. T., Choat, B., Atkin, O. A., Barton, C. V. M. 2018. Trees tolerate an extreme heatwave via sustained transpirational cooling and leaf increased thermal tolerance. *Global Change Biology* 24: 2390-2402.

Gaoua, N. (2010) Cognitive function in hot environments: a question of methodology. *Scandinavian Journal of Medicine and Science in Sports* 20: 60-70.

Gillner, S., Vogt, J., Tharang, A., Dettmann, S., Roloff, A. 2015. Role of street trees in mitigating effects of heat and drought at highly sealed urban sites. *Landscape and Urban Planning* 143: 33-42.

Goodman, J., Hurwitz, M., Park, J., Smith, J. 2018. *Heat and learning*. National Bureau of Economic Research, Working Paper 21639, Cambridge, MA, United States, 53 p.

Harris, F. (2018) Outdoor learning spaces: the case of forest school. *Area* 50: 222-231.

Hanatani, R., Laasko, I., Hirata, A., Kojima, M., Sasaki, H. 2011. Dominant factors affecting temperature elevation in adult and child models exposed to solar radiation in hot environment. *Progress in Electromagnetics Research B* 34: 47-61.

ISO 13732. 2010. *Ergonomics of the thermal environment – methods for the assessment of human responses to contact with surfaces. Part 1: Hot surfaces*. International Organisation for Standardisation, 44 p.

Koc, C. B., Osmond, P., Peters, A. 2018. Evaluating the cooling effects of green infrastructure: A systematic review of methods, indicators and data sources. *Solar Energy 166:* 486-508.

Lafortune, J., Schonholzer, D. 2018. *Do school facilities matter? Measuring the effects of capital expenditures on student and neighbourhood outcomes*. Working Paper, Public Policy Institute of California, San Francisco, CA, United States, 83 p.

Ma, S., Pitman, A., Hart, M., Evans, J., Haghdadi, N., Macgill, I. 2017. The impact of an urban canopy and anthropogenic heat fluxes on Sydney's climate. *International Journal of Climatology* 37: 255-270.

Madden, A., Arora, V., Holmes, K., Pfautsch, S. 2018. *Cool Schools*. Western Sydney University, Parramatta, NSW, Australia, 56 p.

Mohanjerani, A., Bakaric, J., Jeffrey-Bailey, T. 2017. The urban heat island effect, its causes, and mitigation, with reference to the thermal properties of asphalt concrete. *Journal of Environmental Management* 197: 522-538.

Morrison, S., Sims, S. 2014. Thermoregulation in children: exercise, heat stress and fluid balance. *Anatomy and Physiology* 5: 41-55.

Neilson, C., Zimmerman, S. 2014. The effect of school construction on test scores, school enrolment, and home prices. *Journal of Public Economics* 120: 18-31.

Norton, B. A., Coutts, A. M., Livesley, S. J., Harris, R. J., Hunter, A. M., Williams, N. S. 2015. Planning for cooler cities: A framework to prioritise green infrastructure to mitigate high temperatures in urban landscapes. *Landscape and Urban Planning* 134: 127-138.

NSW Department of Education. 2018. *Cooler classrooms for NSW public schools*. Accessed 25 May 2020 at: https://www.nsw.gov.au/news-and-events/news/cooler-classrooms-for-nsw-public-schools/.

Oliveria, S. A., Saraiya, M., Gellner, A. C., Heneghan, M. K., Jorgensen, C. 2006. Sun exposure and risk of melanoma. *Archives of Disease in Childhood* 91: 131-138.

Oliveria, A., Raimundo, A., Gaspar, A., Quintela, D. 2019. Globe temperature and its measurement requirements and limitations. *Annals of Work Exposures and Health* 63: 743-758.

Onori, A., Lavau, S., Fletcher, T. 2018. Implementation as more than installation: a case study of the challenges in implementing green infrastructure projects in two Australian primary schools. *Urban Water Journal* 15: 911-917.

Pfautsch, S., Rouillard, S. 2019A. *Benchmarking heat in Parramatta, Sydney's central river city*. Western Sydney University, Parramatta, NSW, Australia, 56 p.

Pfautsch, S., Rouillard, S. 2019B. *Benchmarking heat across Campbelltown, New South Wales*. Western Sydney University, Parramatta, NSW, Australia, 60 p.

Razzaghmanesh, M., Beecham, S., Salemi, T. 2016. The role of green roofs in mitigating Urban Heat Island effects in the metropolitan area of Adelaide, South Australia. *Urban Forestry and Urban Greening* 15: 89-102.

Ridgers, N., Timperio, A., Crawford, D., Salmon, J. 2013, What factors are associated with adolescent's school break time physical activity and sedentary time? *PLoS One* 8: e56838.

Roach, T., Whitney, J. 2019. *Heat and learning in primary and secondary education*. Department of Economics, University of Central Oklahoma, Edmond, OK, United States, 15 p.

Salamanca, F., Georgescu, M., Mahalov, A., Moustaoui, M, Wang, M. 2014. Anthropogenic heating of the urban environment due to air conditioning. *Journal of Geophysical Research: Atmospheres* 119: 5949-5965.

Sanusi, R., Johnstone, D., May, P., Livesley, S. J. 2017. Microclimate benefits that different street tree species provide to sidewalk pedestrians relate to differences in Plant Area Index. *Landscape and Urban Planning* 157: 502-511.

Seppänen, O., Fisk, W., Lei, Q. H. 2006. *Effect of temperature on task performance in office environment.* Lawrence Berkeley National Laboratory, Berkeley, CA, United States, 11 p.

Snyder, R., Shaw, R. H. 1984. *Converting humidity expressions with computers and calculators*. Division of Agriculture and Natural Resources, University of California, Davis, CA, United States, leaflet 21372.

Teli, D., Bourikas, L., James, P., Bahaj, A. 2017. Thermal performance evaluation of school buildings using a children-based adaptive comfort model. *Procedia Environmental Sciences* 38: 844-851.

Teli, D., Jentsch, M., James, P. 2012. Naturally ventilated classrooms: an assessment of existing comfort models for predicting the thermal sensation and preference of primary school children. *Energy and Buildings* 53: 166-182.

Vanos, J. K. 2015. Children's health and vulnerability in outdoor microclimates: a comprehensive review. *Environment International* 76: 1-15.

Vardoulakis, S., Dear, K., Hajat, S., Heavsde, C., Eggen, B., McMichael, A. 2014. Comparative assessment of the effects of climate change on heat-and-cold related mortality in the United Kingdom and Australia. *Environment and Health Perspectives* 122: 1285-1292.

Wargocki, P., Porras-Salazar, J., Contreras-Espinoza, S. 2019. The relationship between classroom temperature and children's performance in school. *Building and Environment* 157: 197-204.

Yaghoobian, N., Kleissl, J., Krayenhoff, E. 2010. Modelling the thermal effects of artificial turf on the Urban Environment. *Journal of Applied Meteorology and Climatology* 49: 332-345.

Ziter, C. D., Pedersen, E. J., Kucharik, C. J., Turner, M. G. 2019. Scale-dependent interactions between tree canopy cover and impervious surfaces reduce daytime urban heat during summer. *Proceedings of the National Academy of Science of the United States of America* 116: 7575-7580.

CONTACT US

Western Sydney University,
Locked Bag 1797, Penrith, NSW 2751

WESTERNSYDNEY.EDU.AU